Planet Formation – The Evidence from The Kuiper Belt

Wladimir Lyra

New Mexico State University

Current Funding

AAG – 2020, 2021

XRP - 2023
EW – 2021, 2022, 2023
TCAN – 2020

Computational Facilities

Australian National University - Mar 13th, 2024

Circumstellar/Protoplanetary Disks

PP disk fact sheet

Density: $10^{13} – 10^{15}$ cm^{-3}
(Air: 10^{21} cm^{-3})

Temperature: 10-1000 K

Scale: 0.1-100AU

Mass: $10^{-3} – 10^{-1}$ M_{sun}

Composition: 5:2 H_2-He mixture. 1% metals.

Planet Formation

"Planets form in disks of gas and dust"

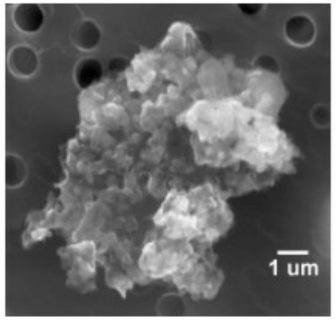

A miracle happens

Dust evolution

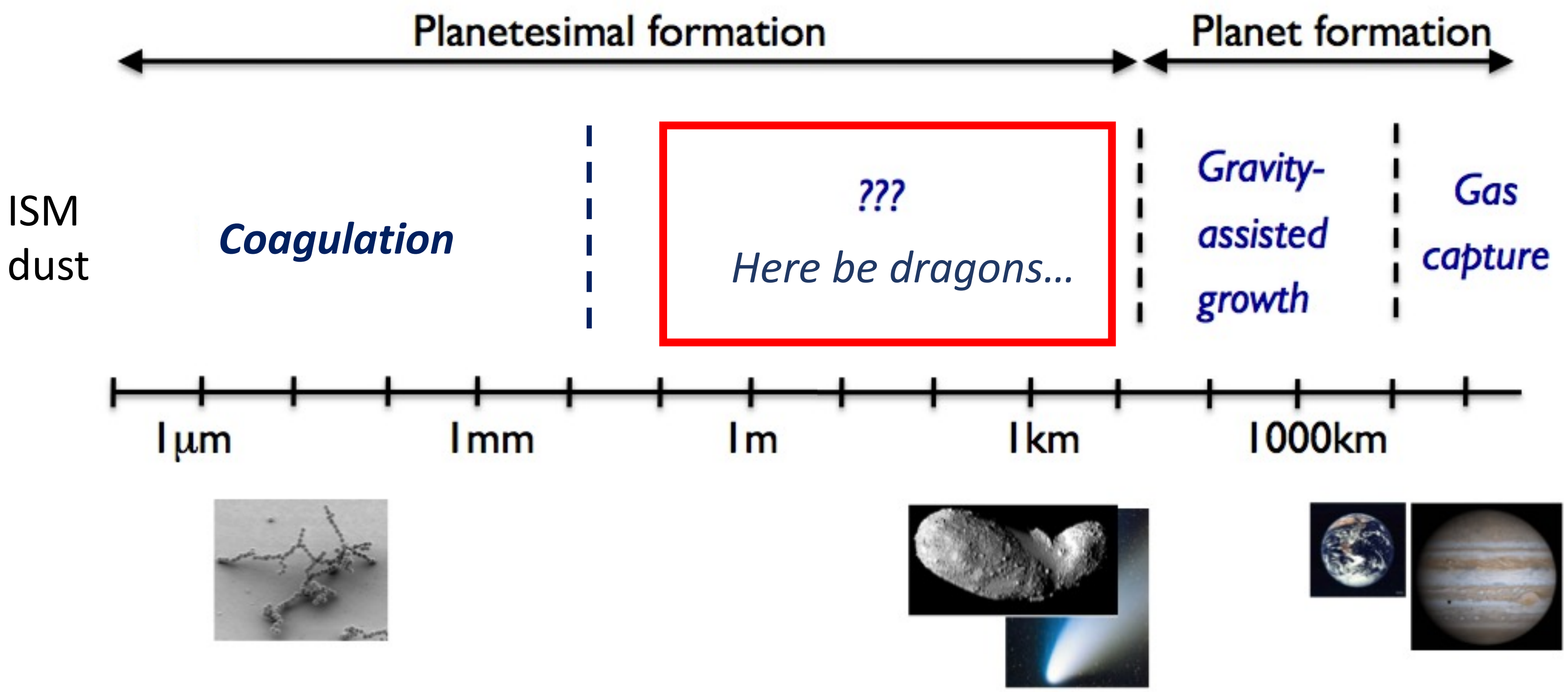

Headwind and Dust Drift

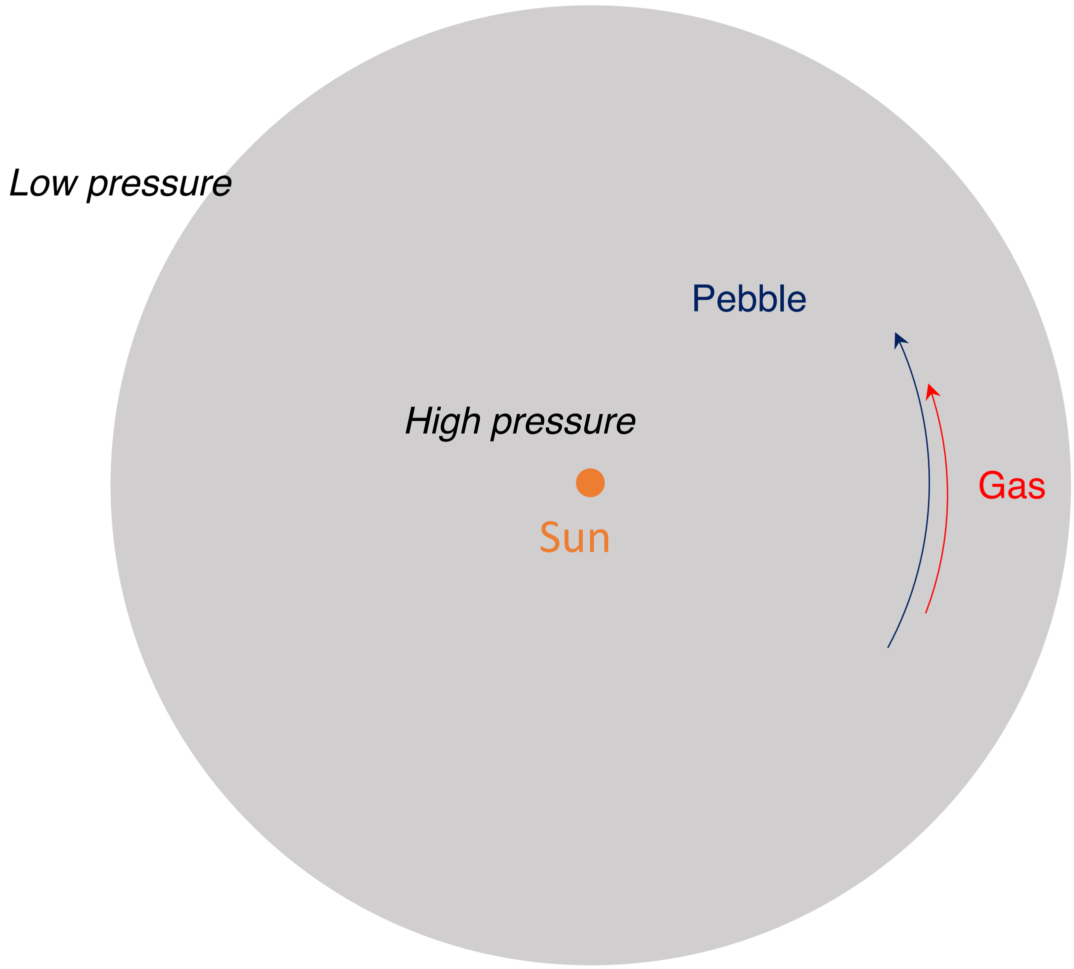

The gas has some pressure support (sub-Keplerian).

The pebbles do not feel gas pressure (Keplerian).

Dust coagulation and drift

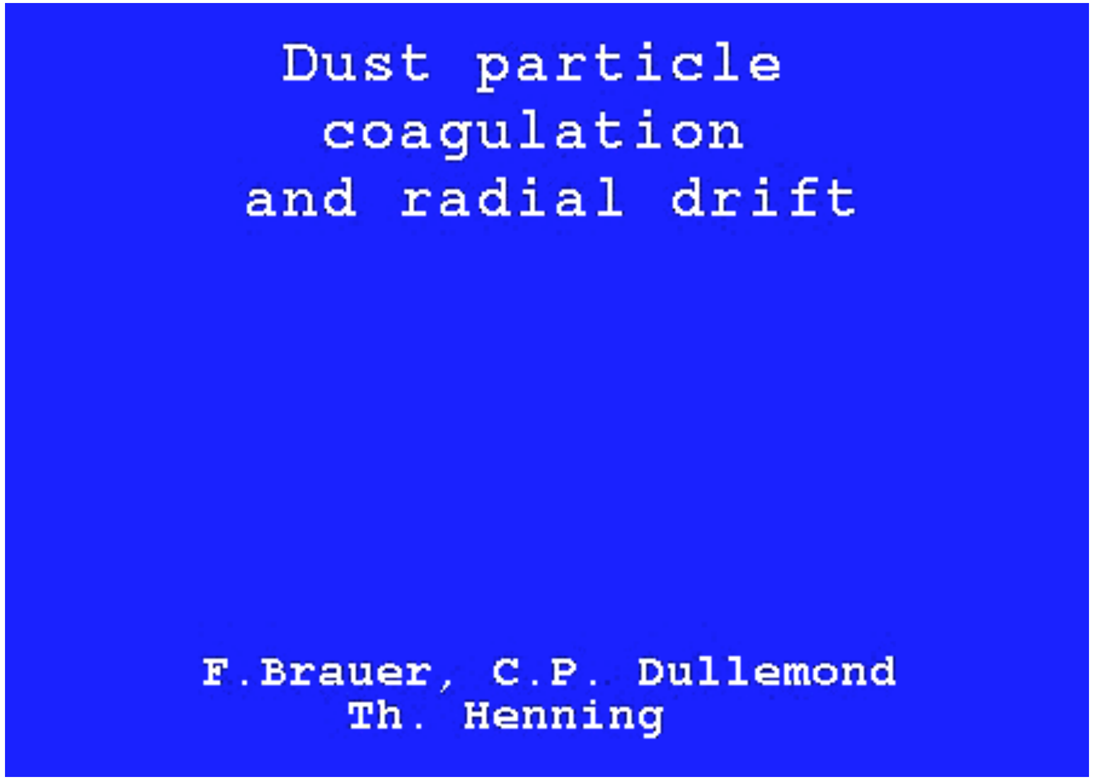

Brauer et al. (2008)

Streaming Instability

The dust drift is hydrodynamically unstable

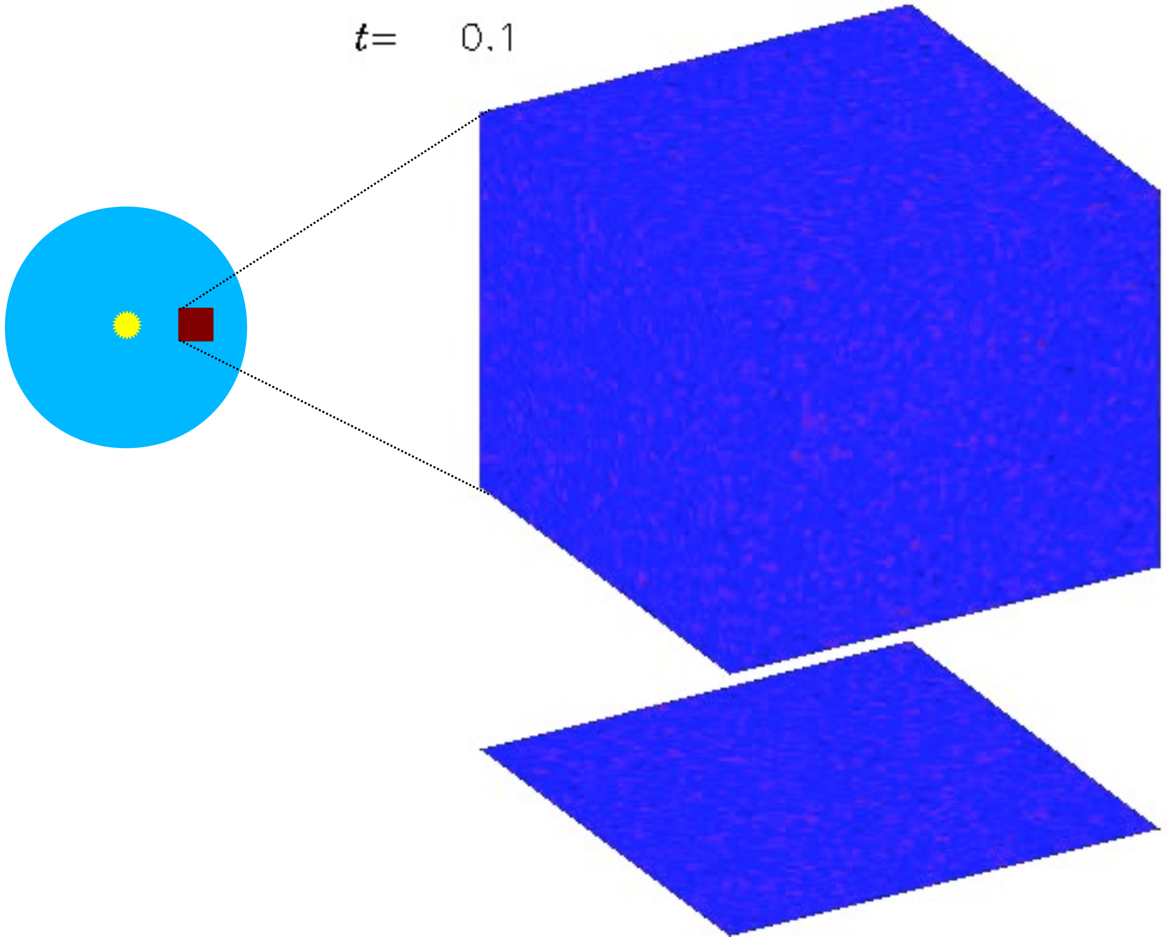

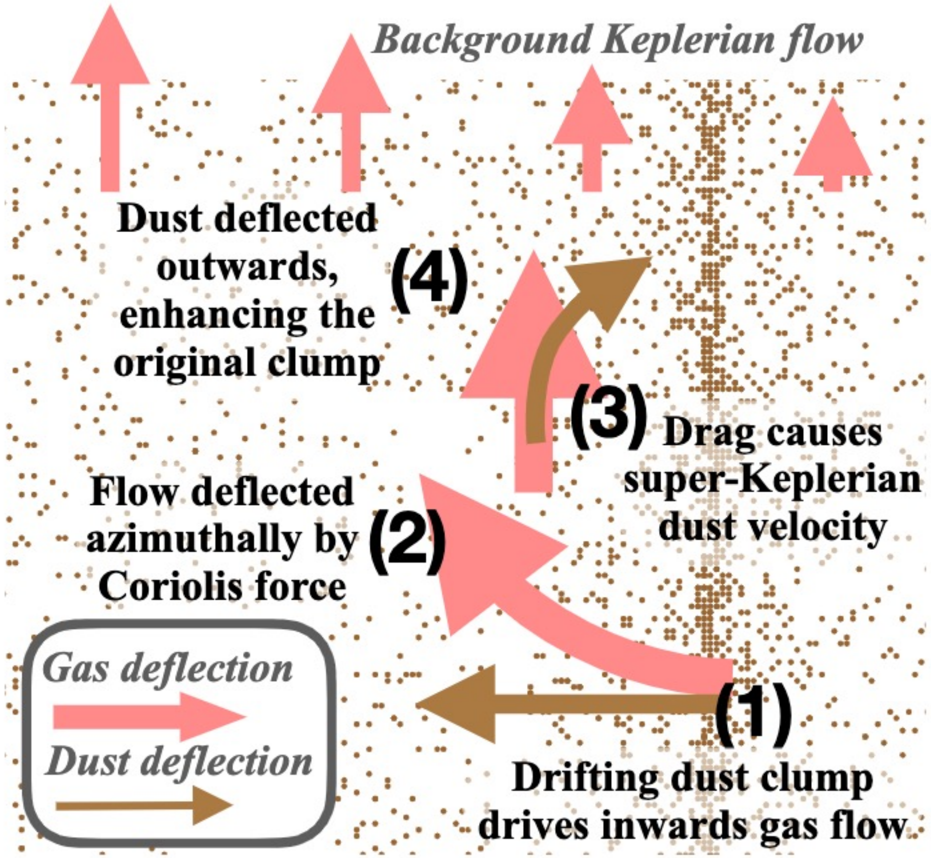

Lesur et al. (2022)

Youdin & Goodman ‘05, Johansen & Youdin ‘07, Youdin & Johansen+ ‘07, Kowalik+ ’13, Lyra & Kuchner ‘13, Schreiber+ ‘18, Klahr & Schreiber ’20, Simon+ ‘16, ‘17, Carrera+ ‘15, ‘17, ‘20, Gole+ ’20, Li+ ‘18, ‘19, Abod+ ’19, Nesvorny+ ’19

Gravitational collapse into planetesimals

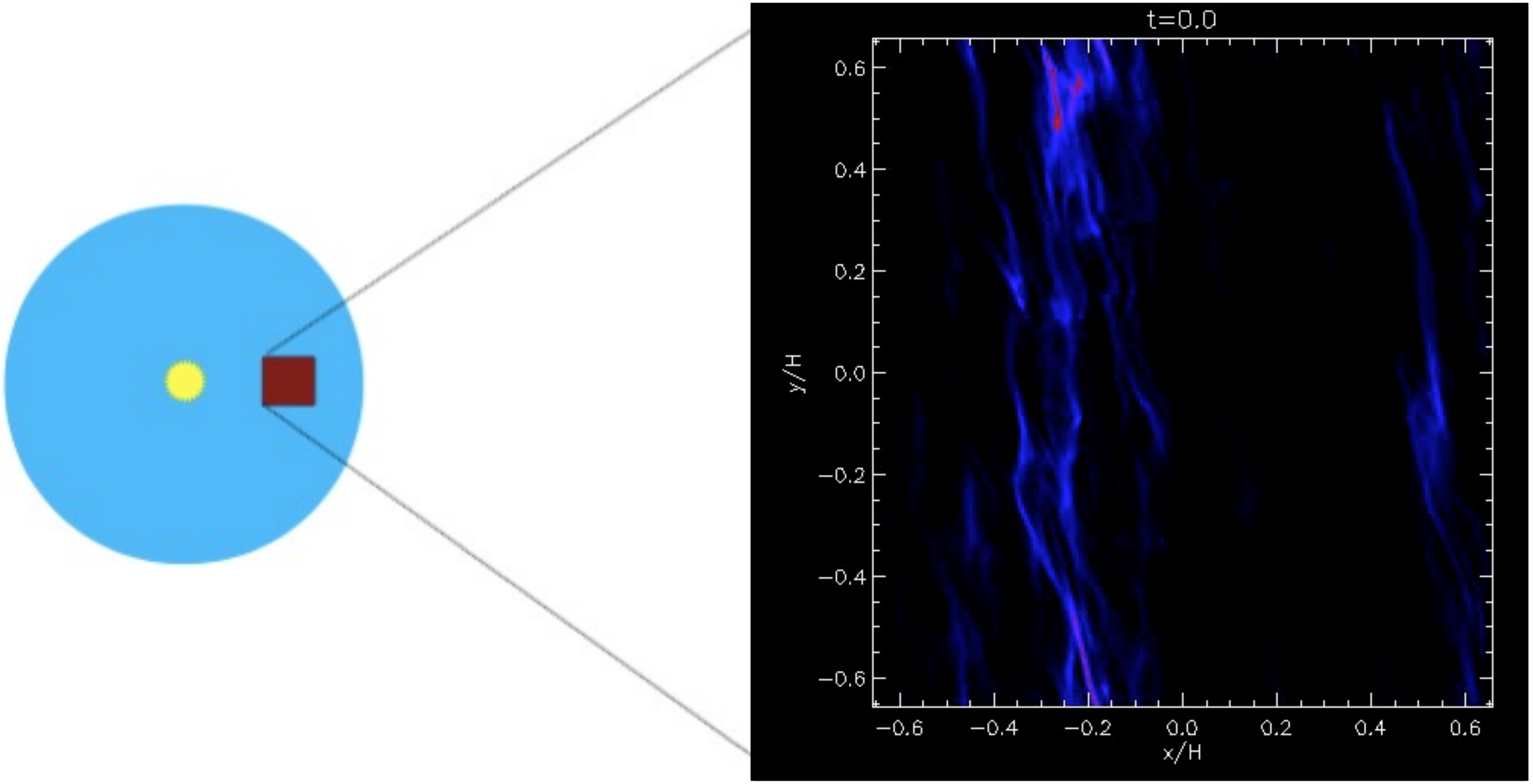

Johansen et al. (2007)

How can we verify the streaming instability hypothesis?

Planetesimal Formation

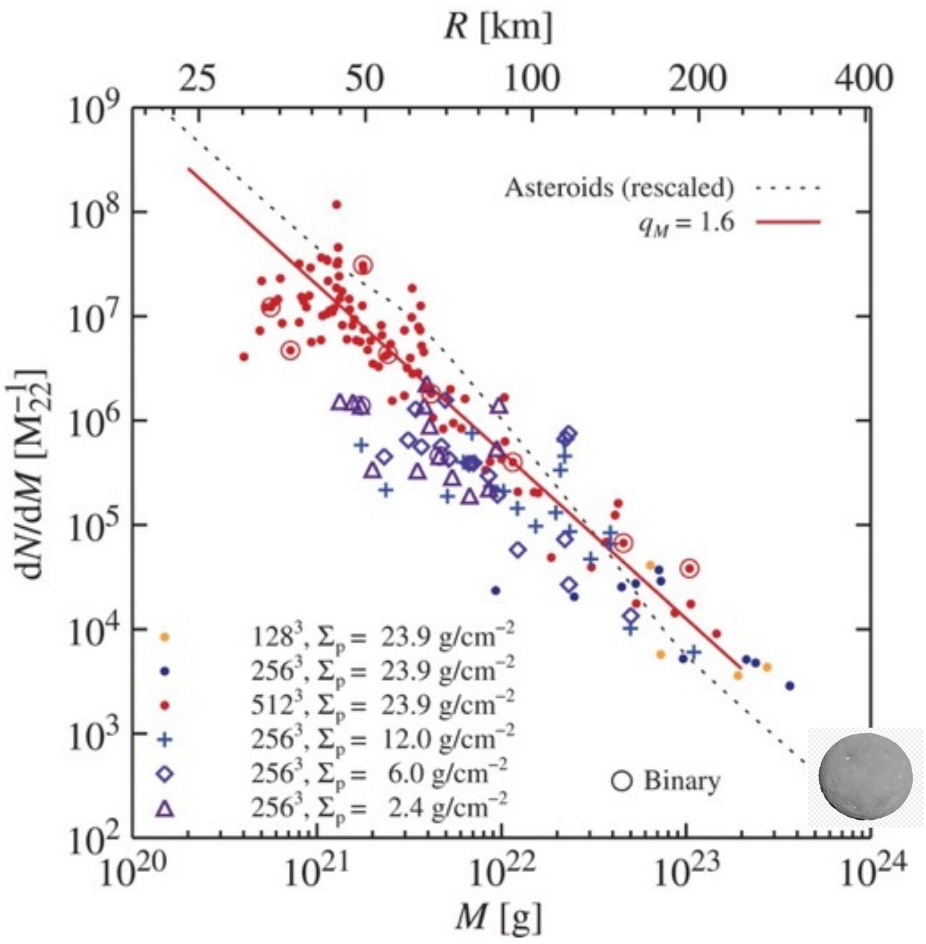

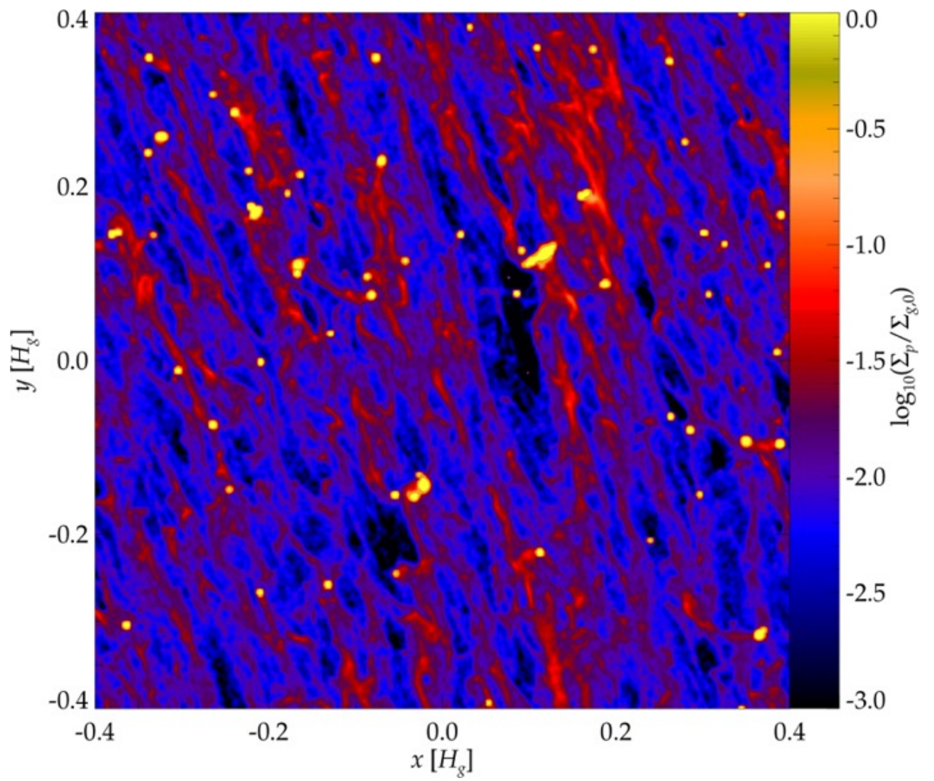

Initial mass function consistent with mass distribution of asteroid belt. Slope 1.6

Yang & Johansen (2014); Schäfer, Yang, & Johansen (2017)

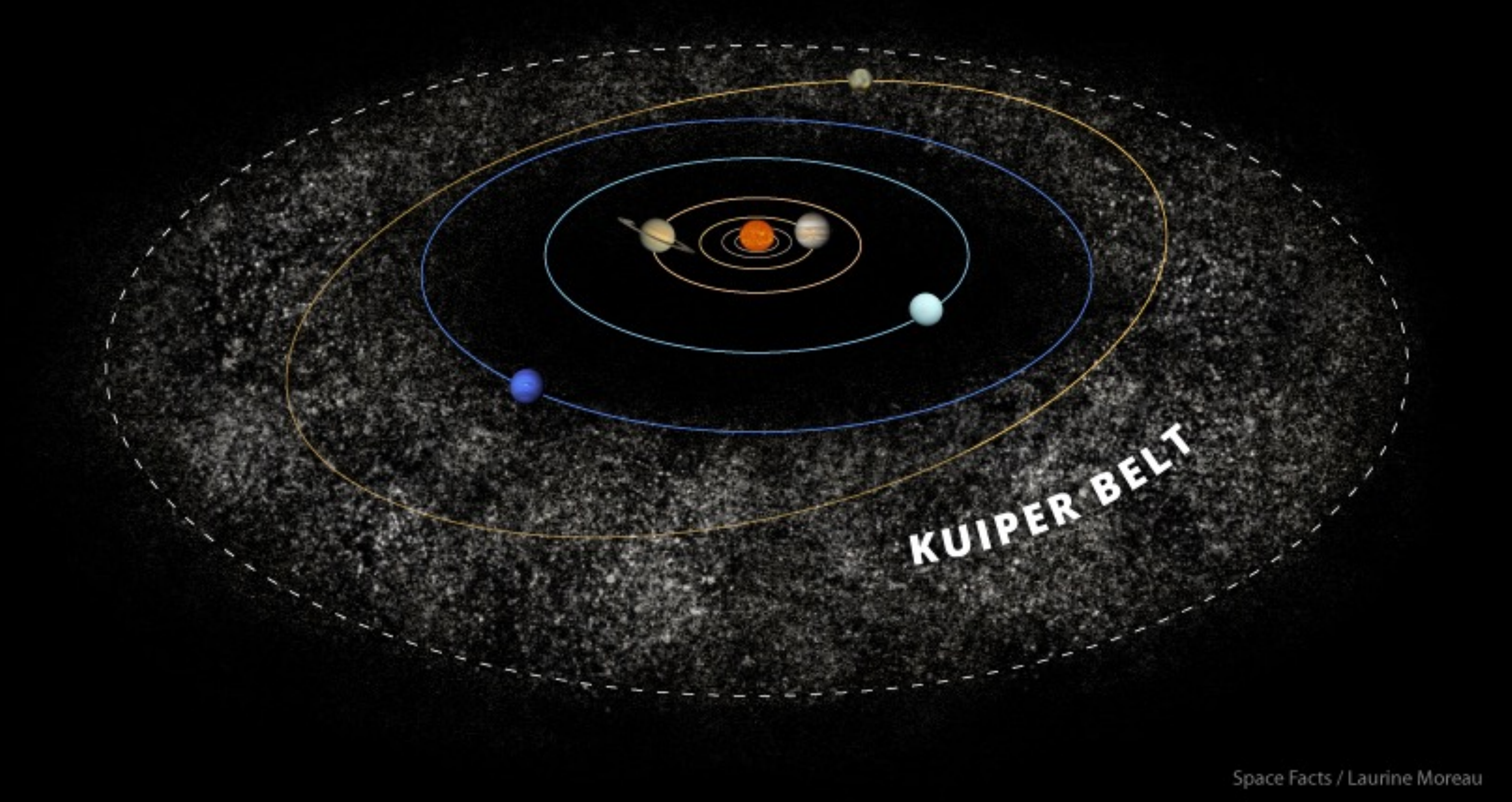
KUIPER BELT
Space Facts / Laurine Moreau

Structure of the Kuiper Belt

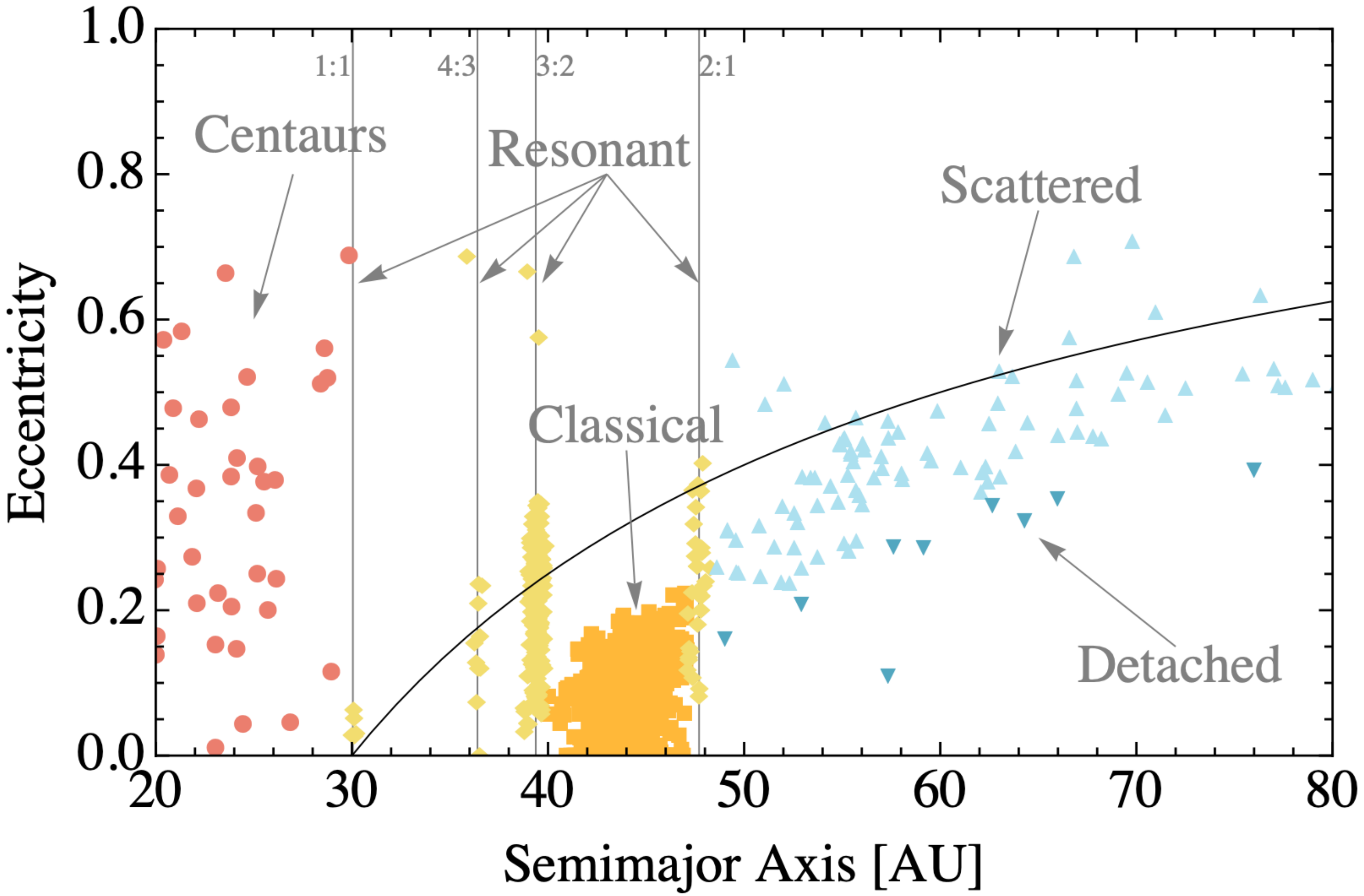

Gladman+ ‘08, Lacerda ‘09, Batygin+ ’10, Dawson & Murray-Clay ‘12

Structure of the Kuiper Belt

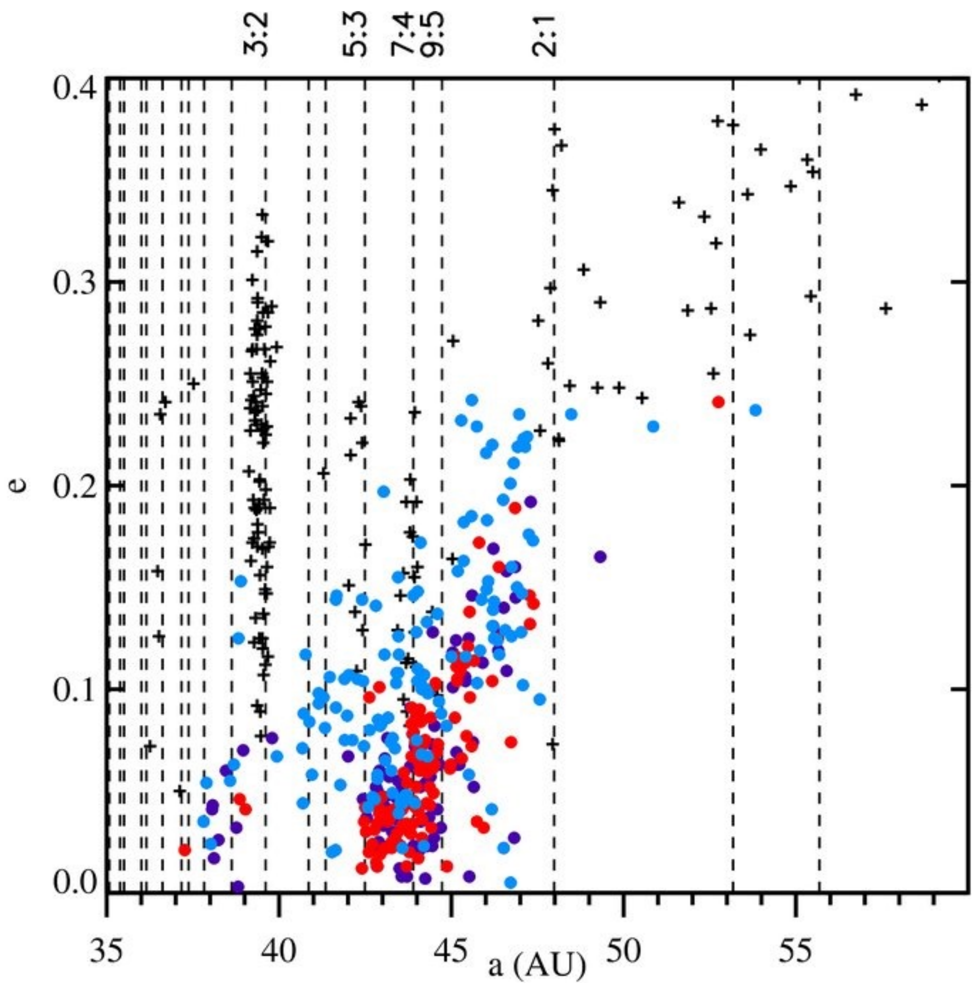

+ Resonant and Scattered
Cold Classical *i*<2°
"Ambiguous" 2°<*i*<6°
Hot Classicals i>6°

Cold Classicals: Presumably pristine planetesimals

Gladman+ '08, Lacerda '09, Batygin+ '10, Dawson & Murray-Clay '12

Arrokoth (MU_{69})

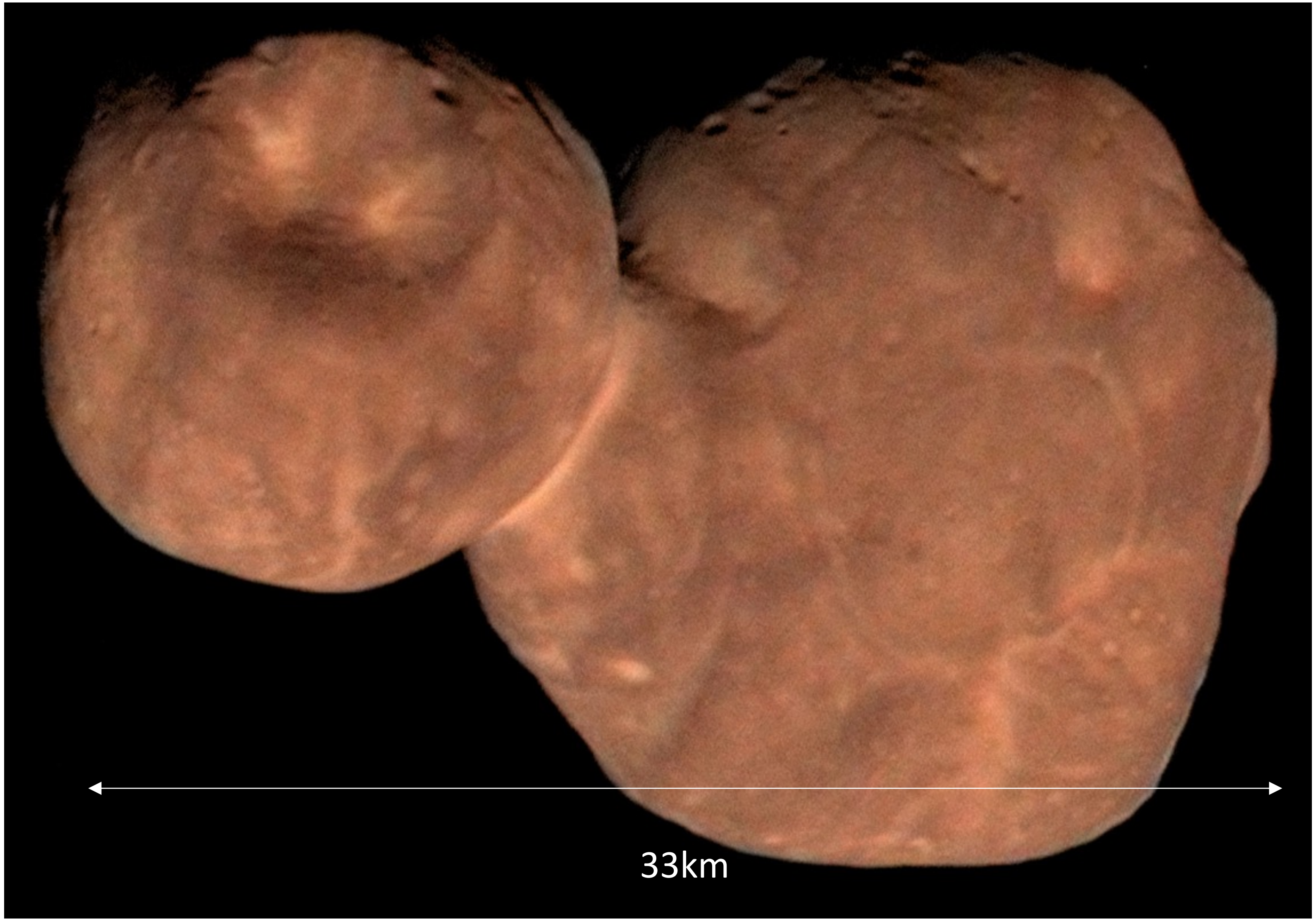

New Horizons Flyby, Jan 2019

The Cartoon Image

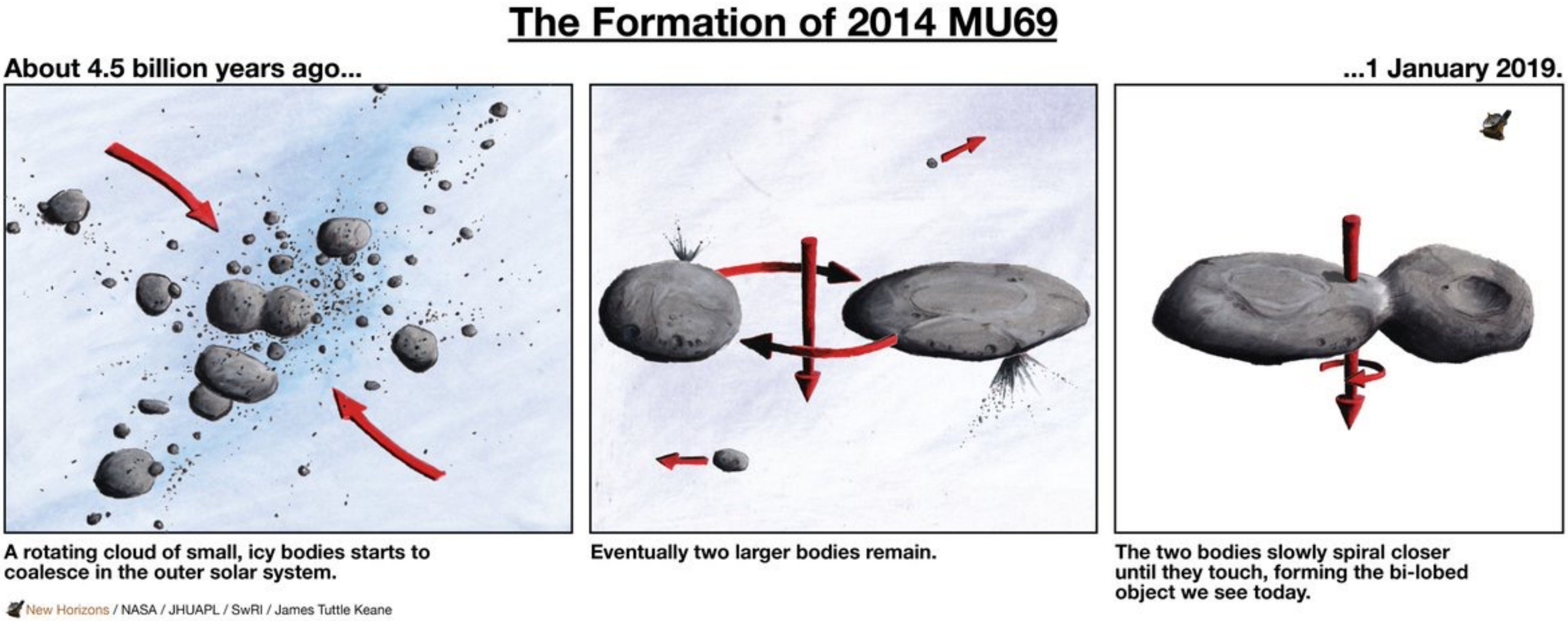

Sketch by J.T. Keane

Arrokoth and Pluto ices are different

Arrokoth : Methanol, H_20, HCN

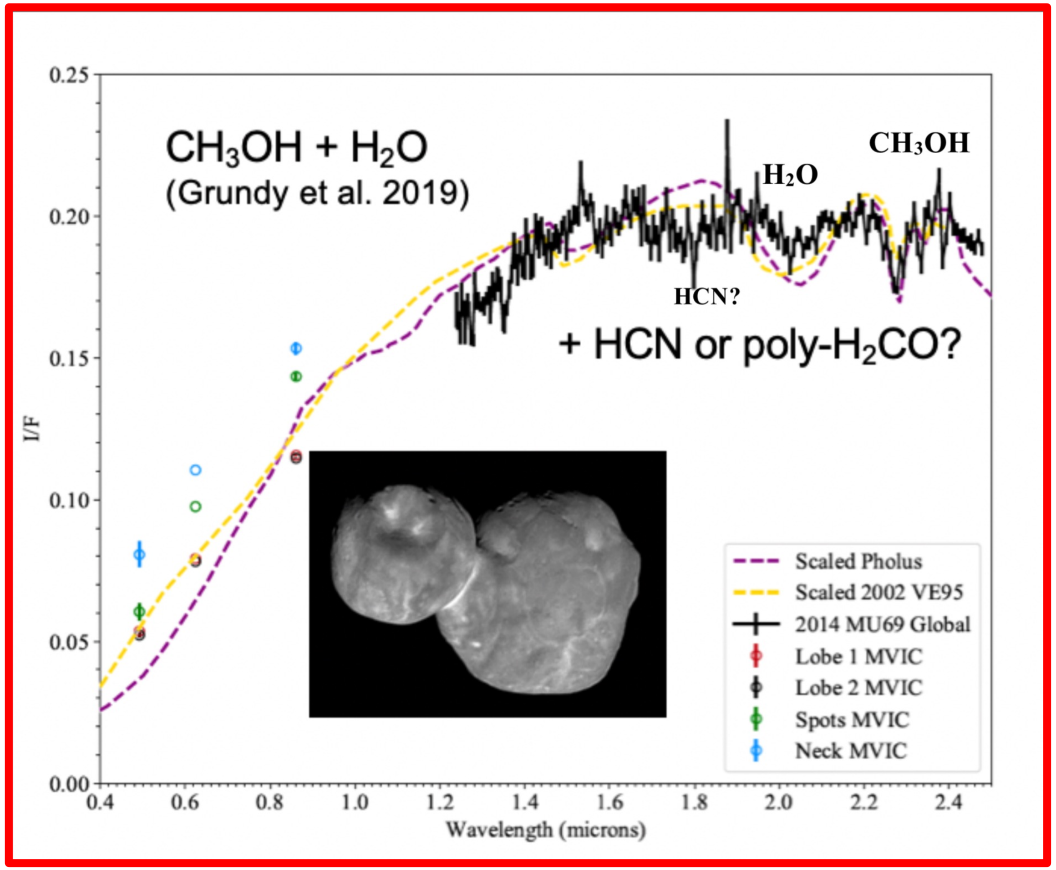

Pluto : CH_4, N_2, CO

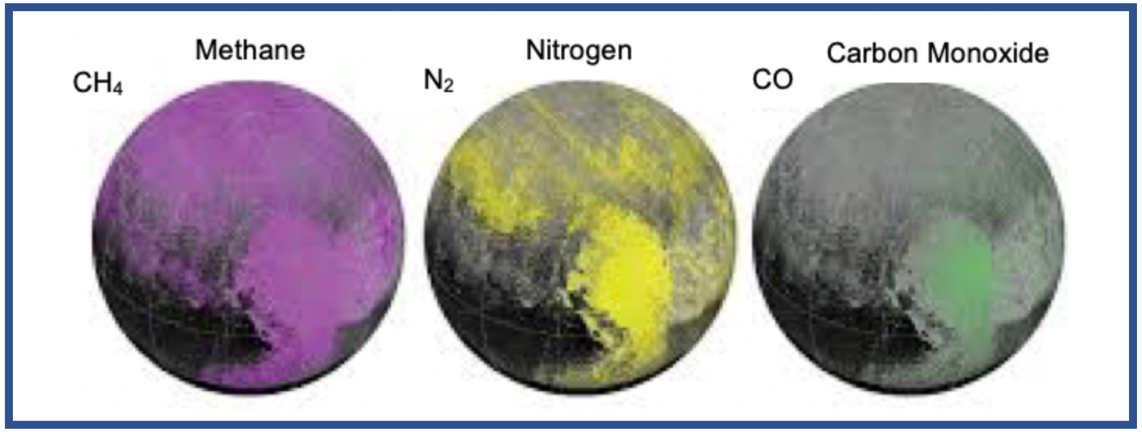

Grundy+ '16, Lisse+Lyra '20

Retention of volatiles

If Pluto is formed from similar bodies to Arrokoth, they must retain volatiles

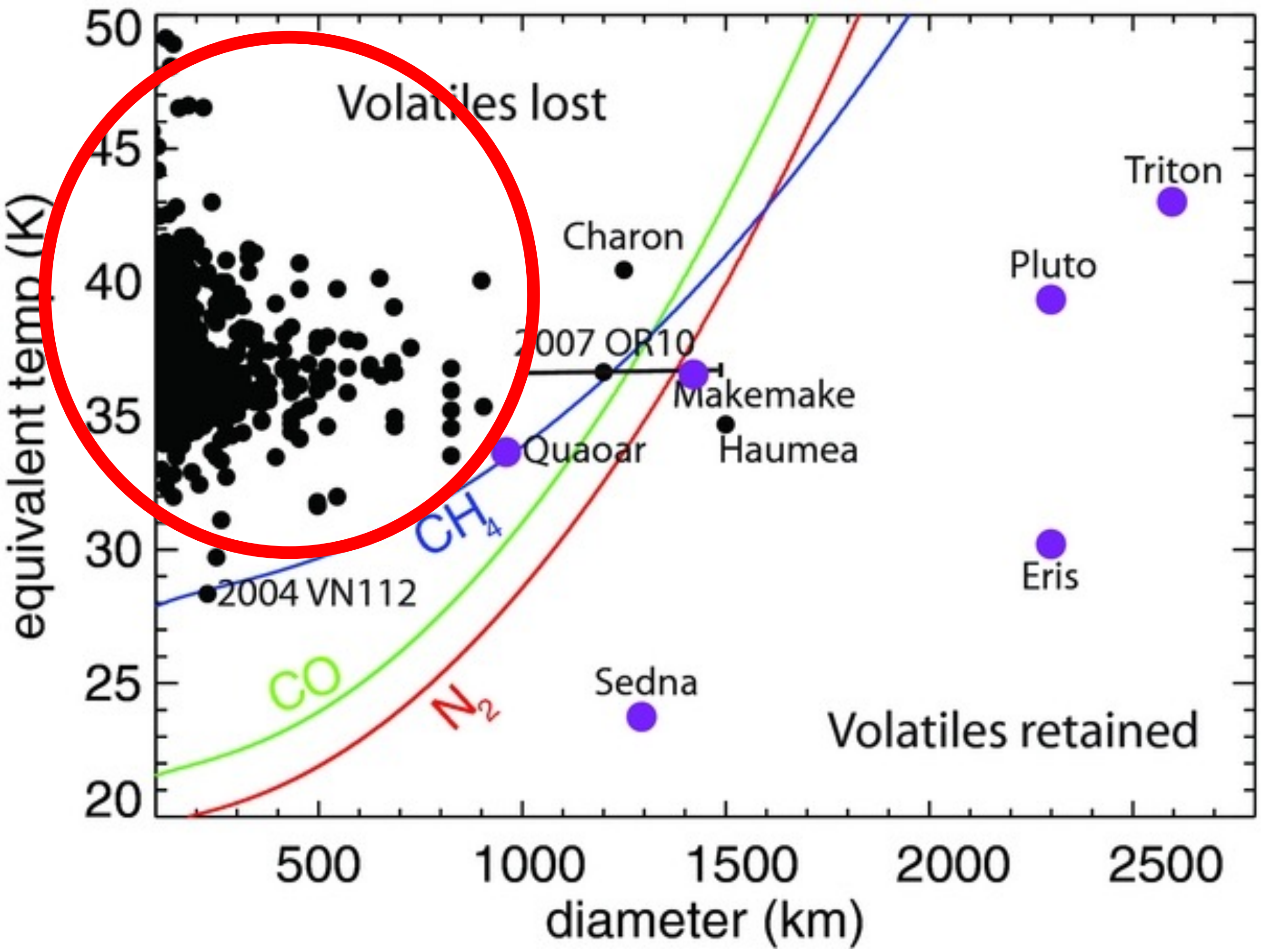

Needs shielding from sunlight

Brown, Burgasser, & Fraser (2011); Lisse+Lyra ‘20

Retention of volatiles

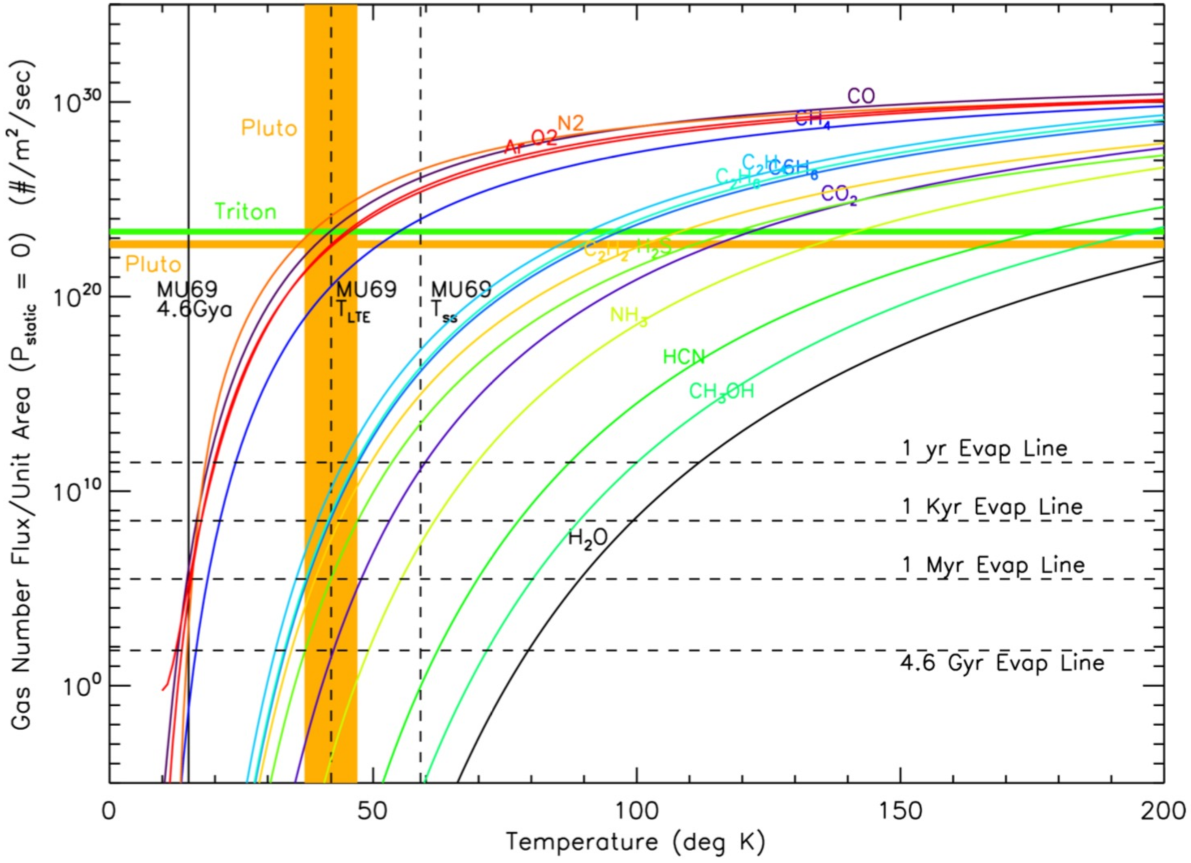

Hypervolatiles (CH_4 / CO / N_2) lost under vacuum pressure and microgravity in ~1 Myr for 40 K

Retained for long times if formed < 20K

Formation of MU69 in an optically thick disk keeps the interior cold enough to allow the volatiles to remain frozen.

Lisse+Lyra ’20

Cold Classical KBOs: Preference for Prograde

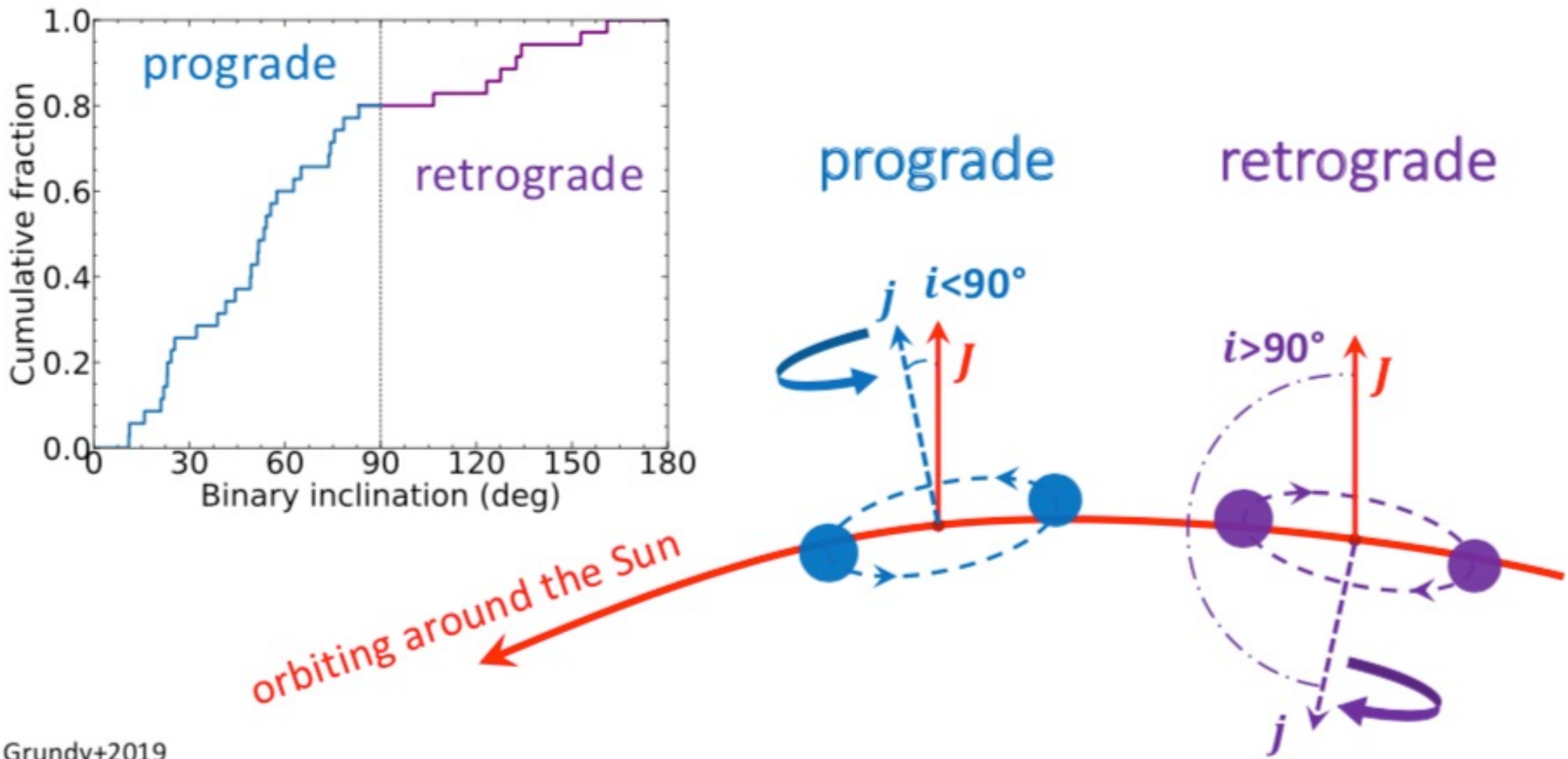

Grundy+2019

Counting binaries: Preference for Prograde (~80%)

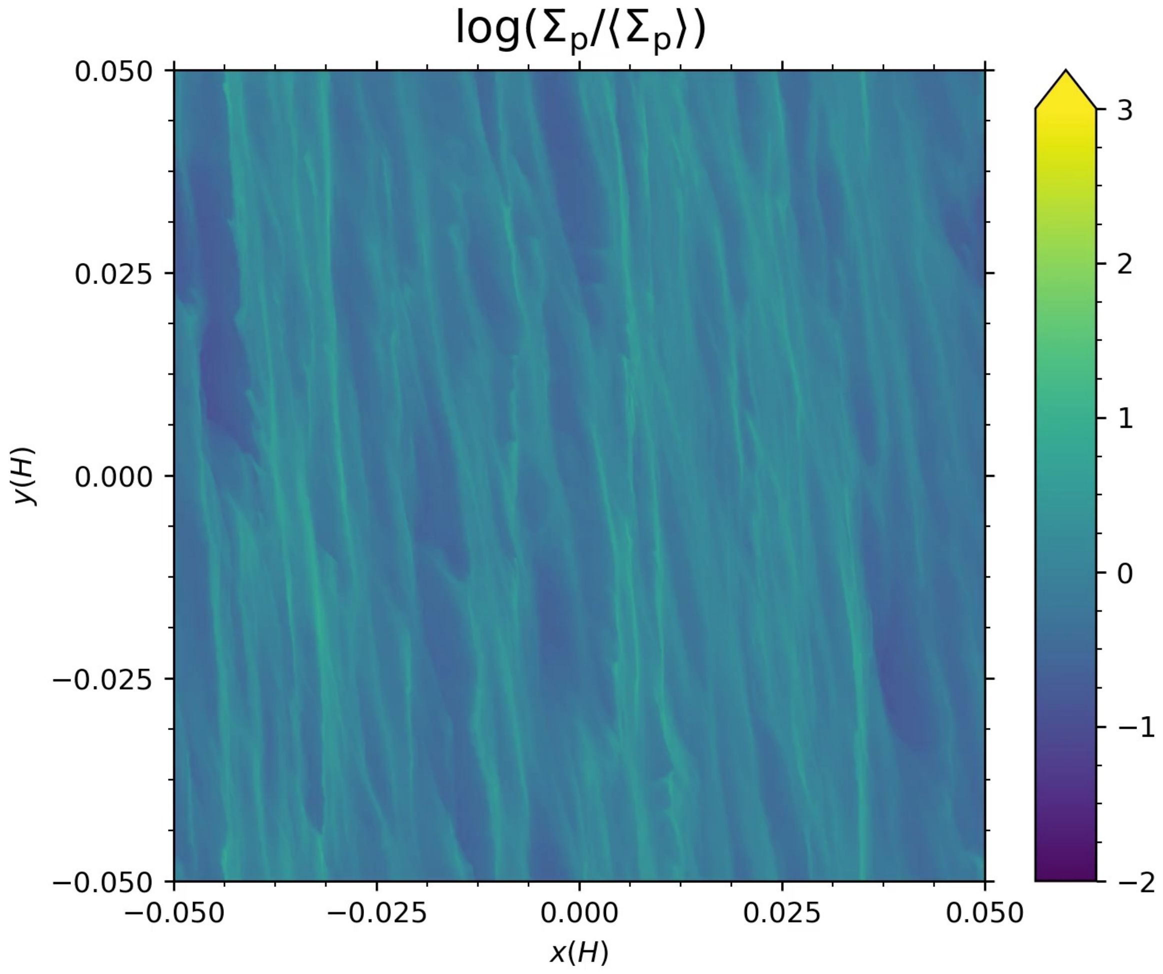

SI Model (solid)
KBOs (dashed)

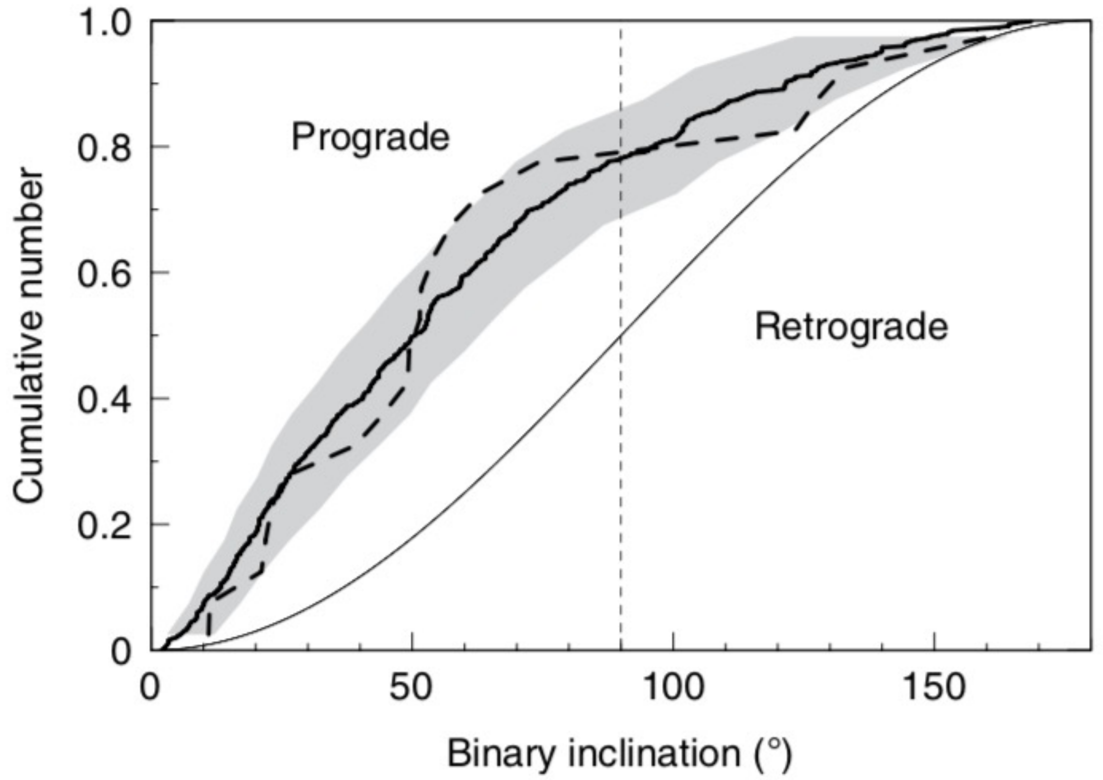

Nesvorny+’19, model by Rixin Li

W. Lyra

How did contact happen?

Mutual orbit
(i.e., not captured)

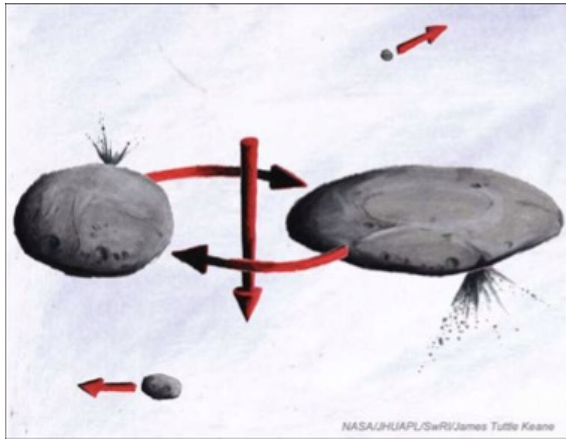

Inferred from:
alignment of component minor axes,
small angular momentum,
similar colors.

Slow merger
(~2 m/s: human walking speed)

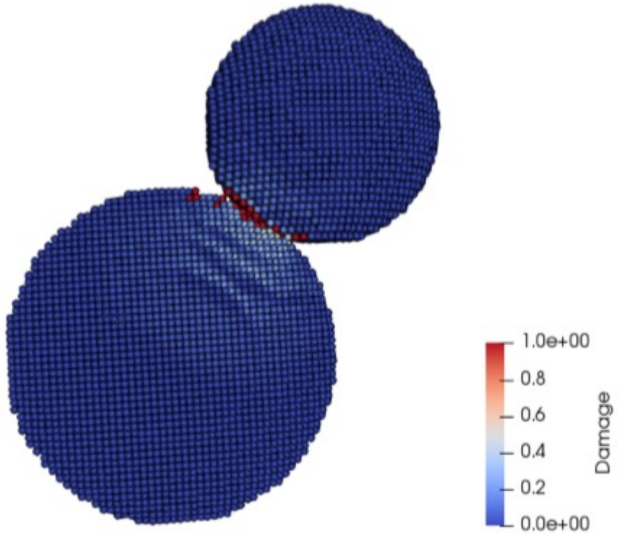

Inferred from:
Negligible evidence for impact damage

Arrokoth (MU_{69})

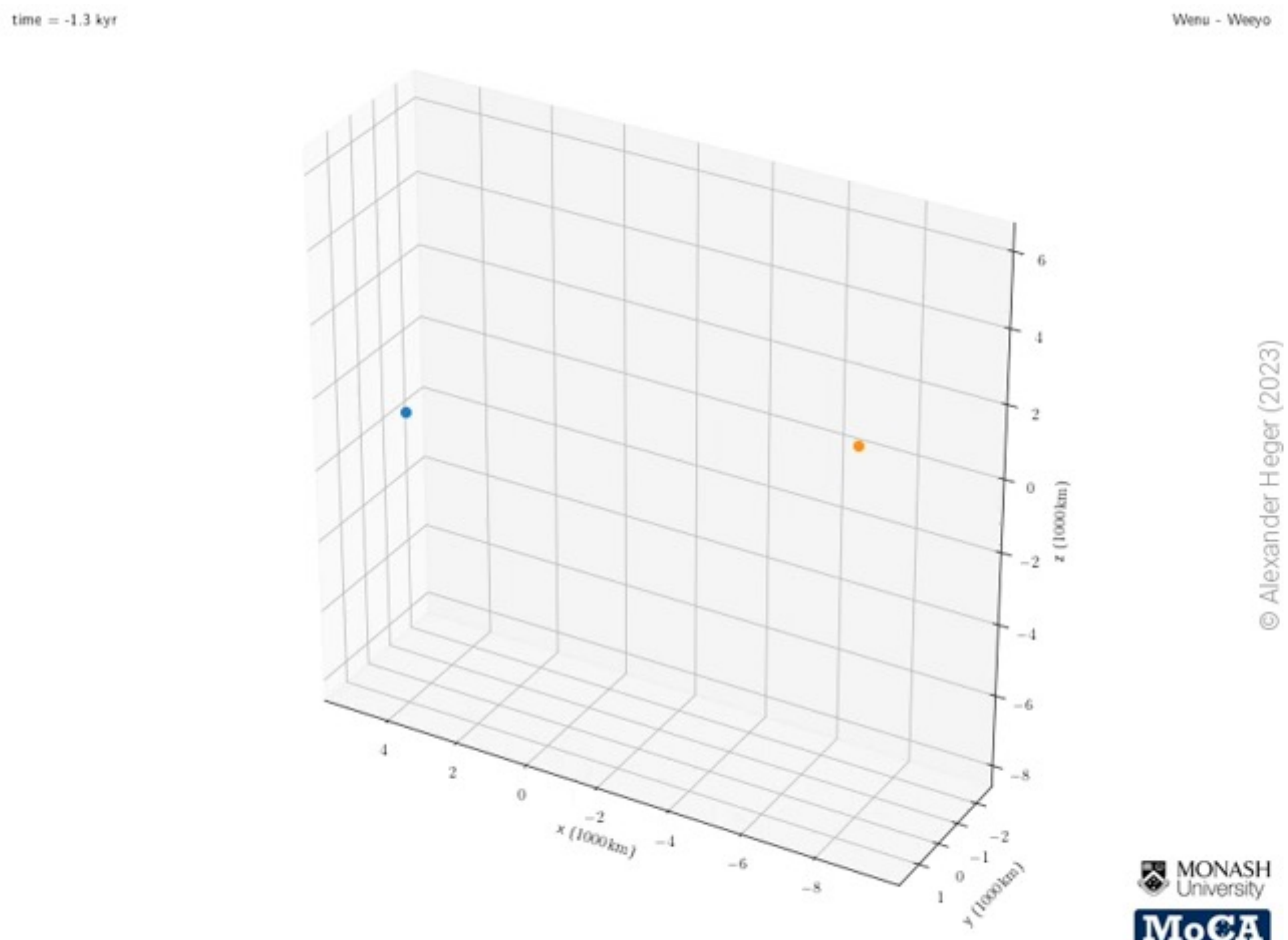

Heger, based on Grishin et al. (2020)

Kozai-Lidov Oscillations

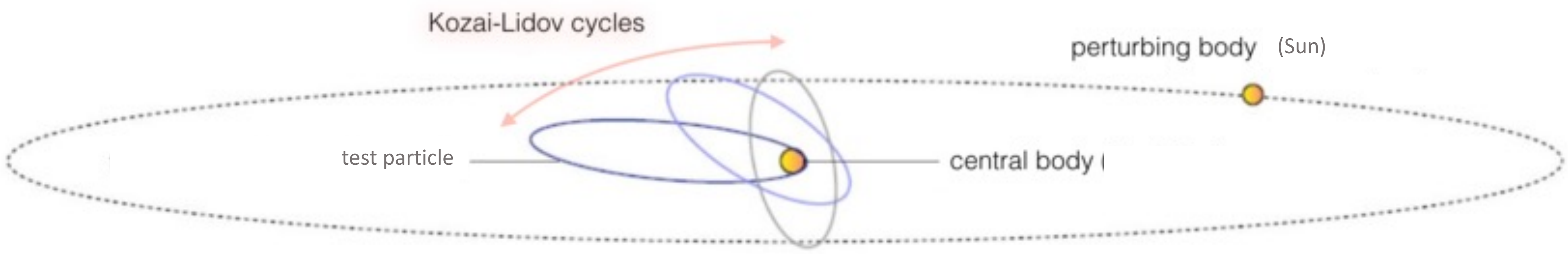

Kozai + Tidal Friction + Permanent Quadrupole + Drag

$$
\begin{aligned}
\frac{de}{dt} &= -e\left[V_1 + V_2 + V_d + 5\left(1-e^2\right)S_{eq}\right],\\
\frac{dh}{dt} &= -h\left(W_1 + W_2 + W_d - 5e^2 S_{eq}\right),\\
\frac{d\hat{e}}{dt} &= \left[Z_1 + Z_2 + \left(1-e^2\right)\left(4S_{ee} - S_{qq}\right)\right]\hat{q}\\
&\quad - \left[Y_1 + Y_2 + \left(1-e^2\right)S_{qh}\right]\hat{h},\\
\frac{d\hat{h}}{dt} &= \left[Y_1 + Y_2 + \left(1-e^2\right)S_{qh}\right]\hat{e}\\
&\quad - \left[X_1 + X_2 + \left(4e^2+1\right)S_{eh}\right]\hat{q},\\
\frac{d\boldsymbol{\Omega}_1}{dt} &= \frac{\mu_r h}{I_1}\left(-Y_1\hat{e} + X_1\hat{q} + W_1\hat{h}\right),\\
\frac{d\boldsymbol{\Omega}_2}{dt} &= \frac{\mu_r h}{I_2}\left(-Y_2\hat{e} + X_2\hat{q} + W_2\hat{h}\right).
\end{aligned}
$$

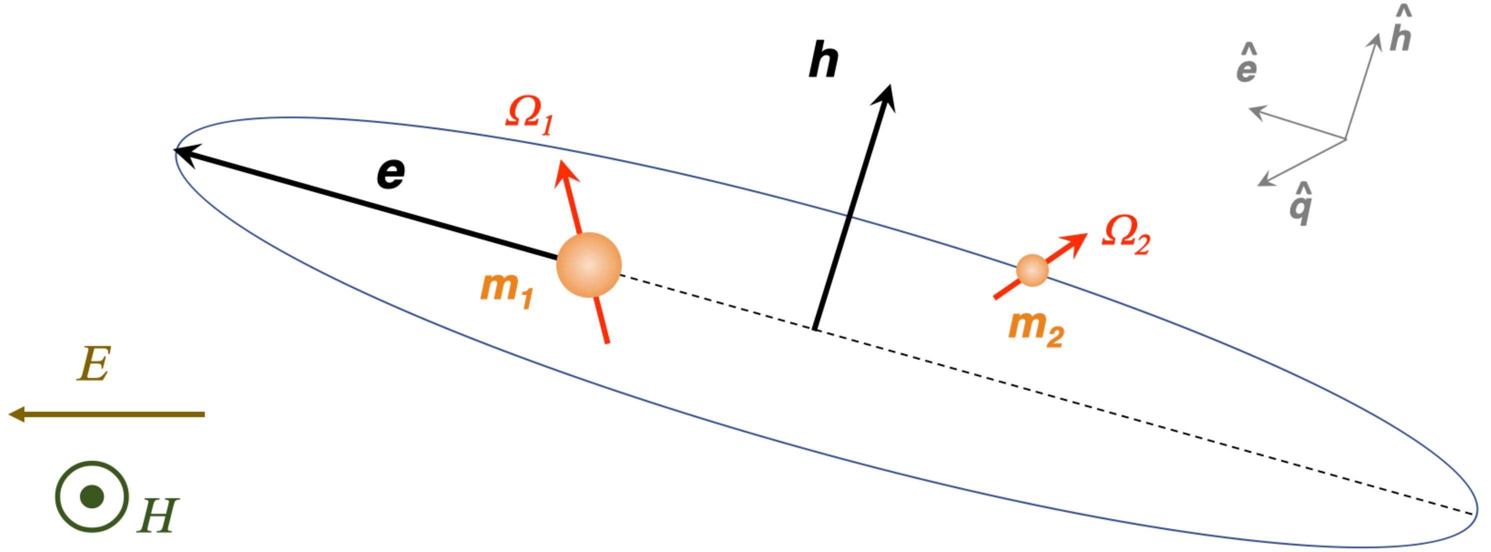

Lyra et al. (2021)

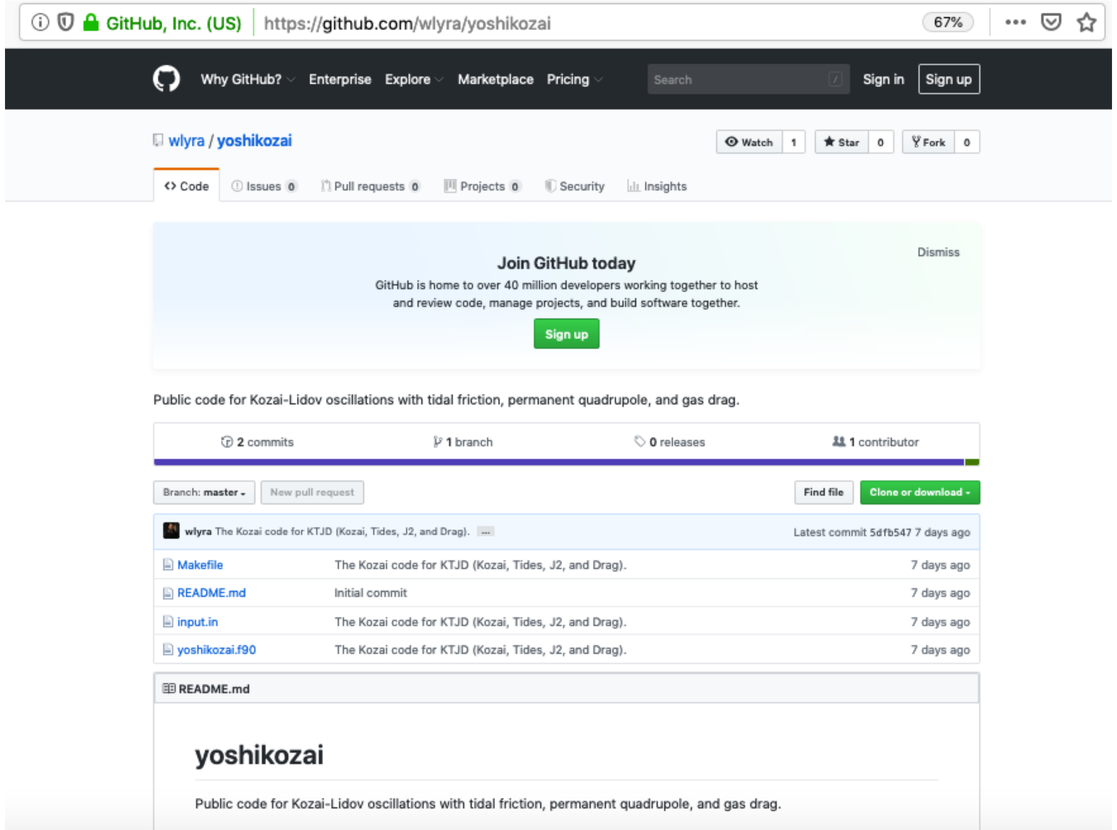

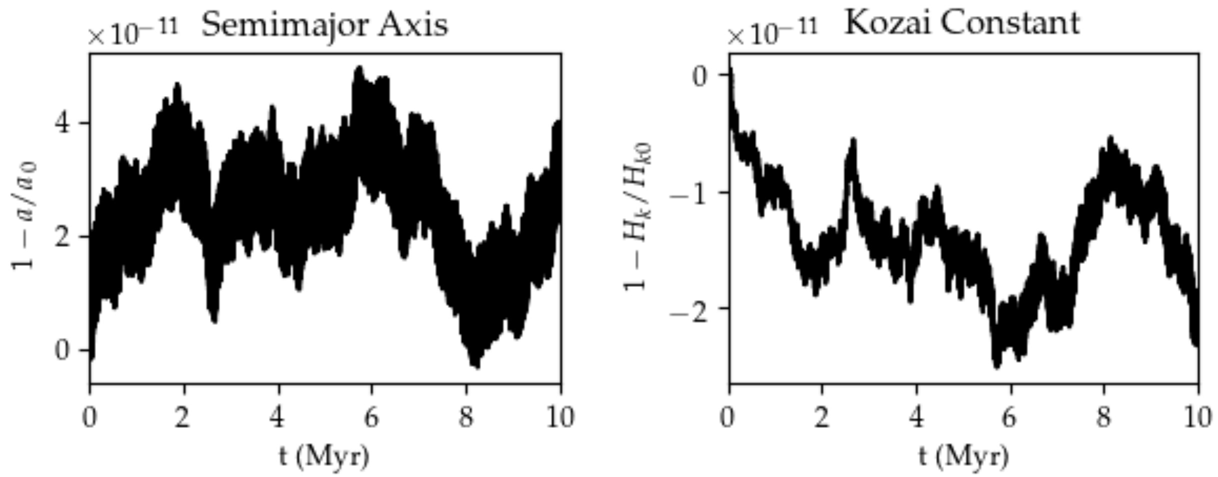

Lyra et al. (2021)

Critical Inclination

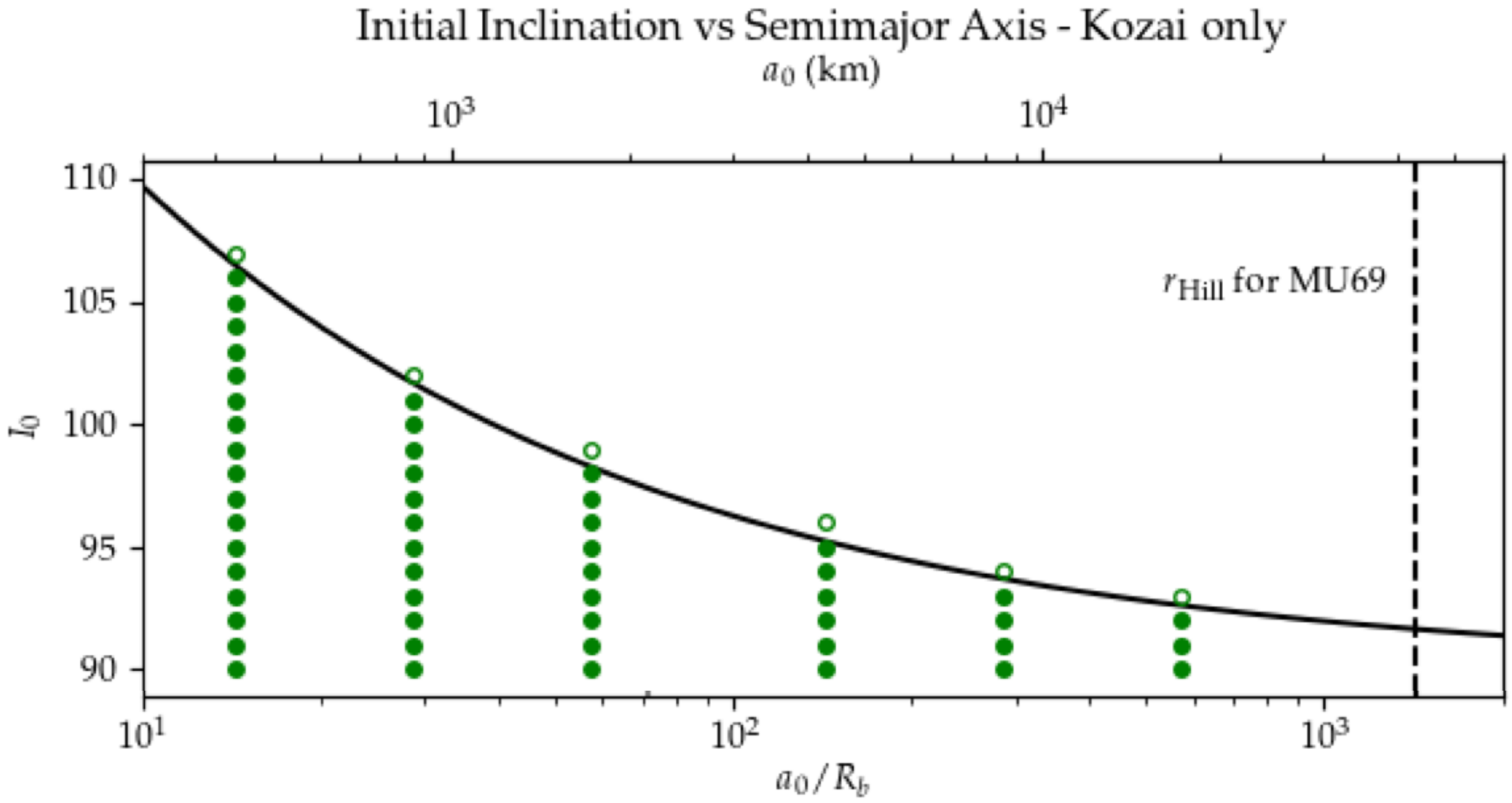

Lyra et al. (2021)

Kozai + Tidal Friction + Permanent Quadrupole + Drag

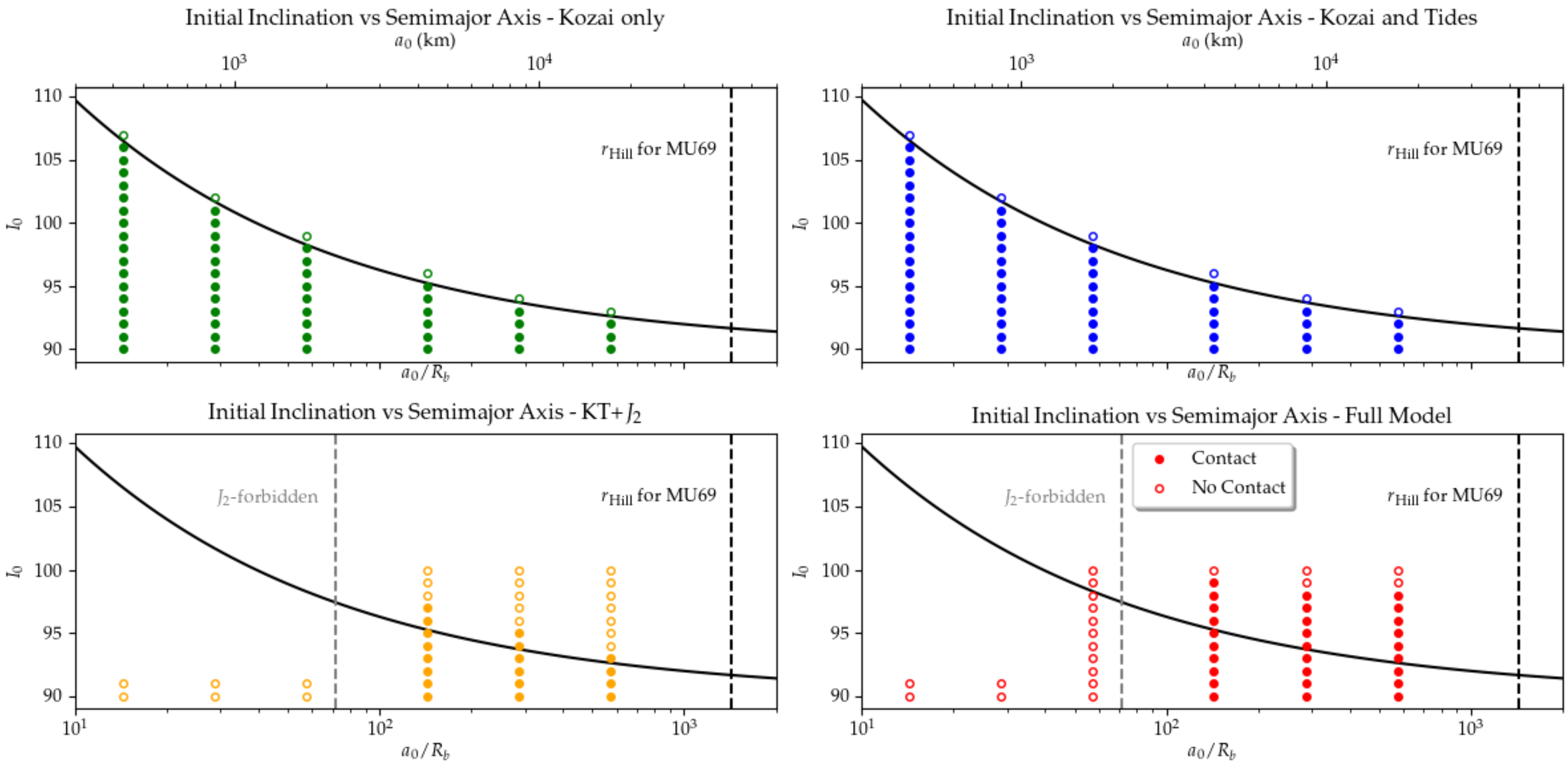

Lyra et al. (2021)

Effect of Drag

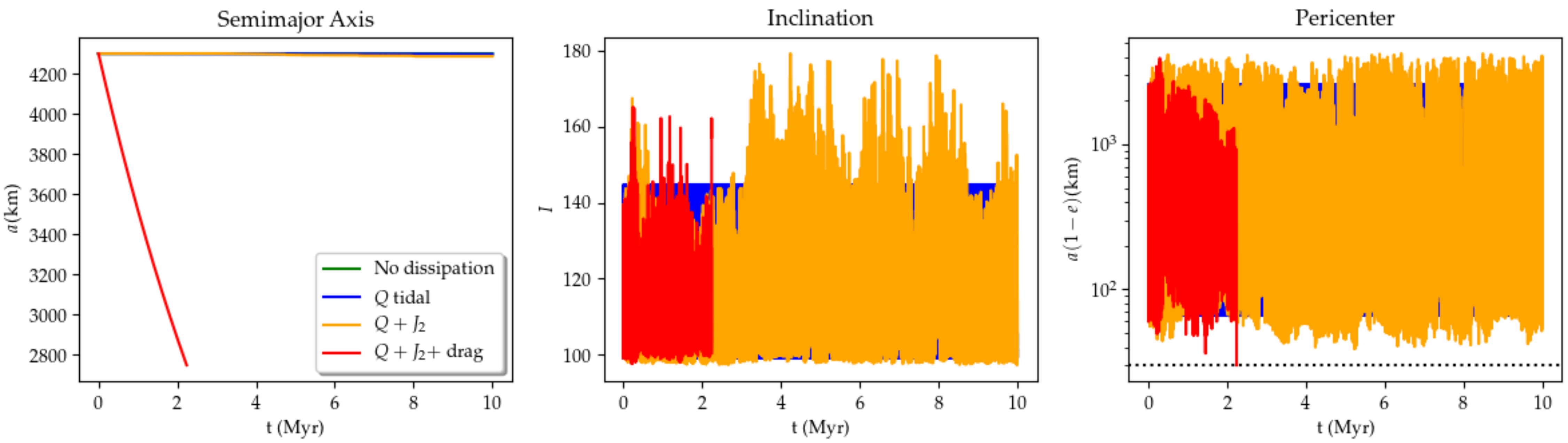

Lyra et al. (2021)

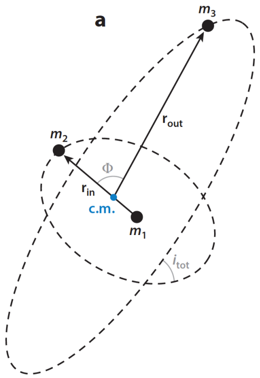

Caveat: limited by double-averaging

Double-Averaged vs Single-Averaged

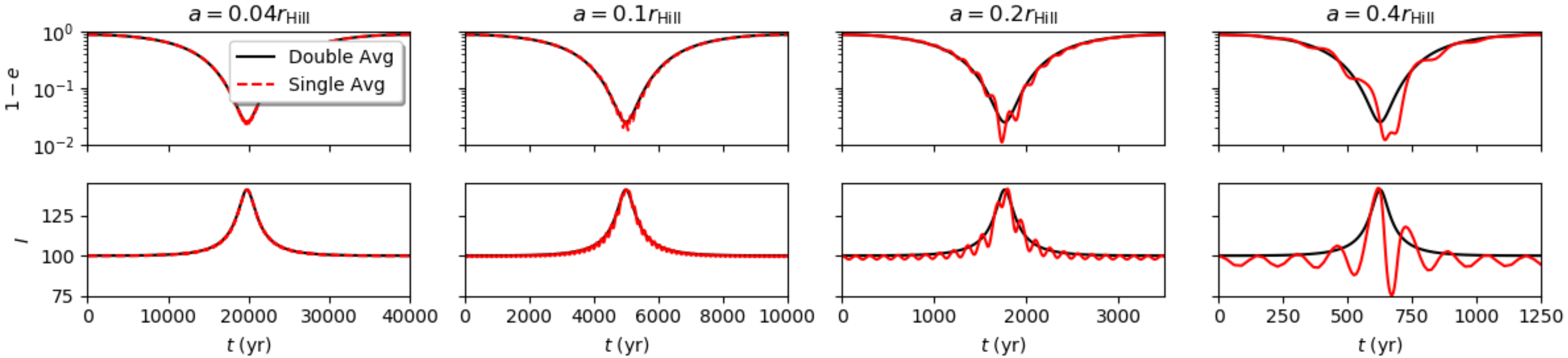

Lyra et al 2021

N-body simulations (no tides, J2, or drag)

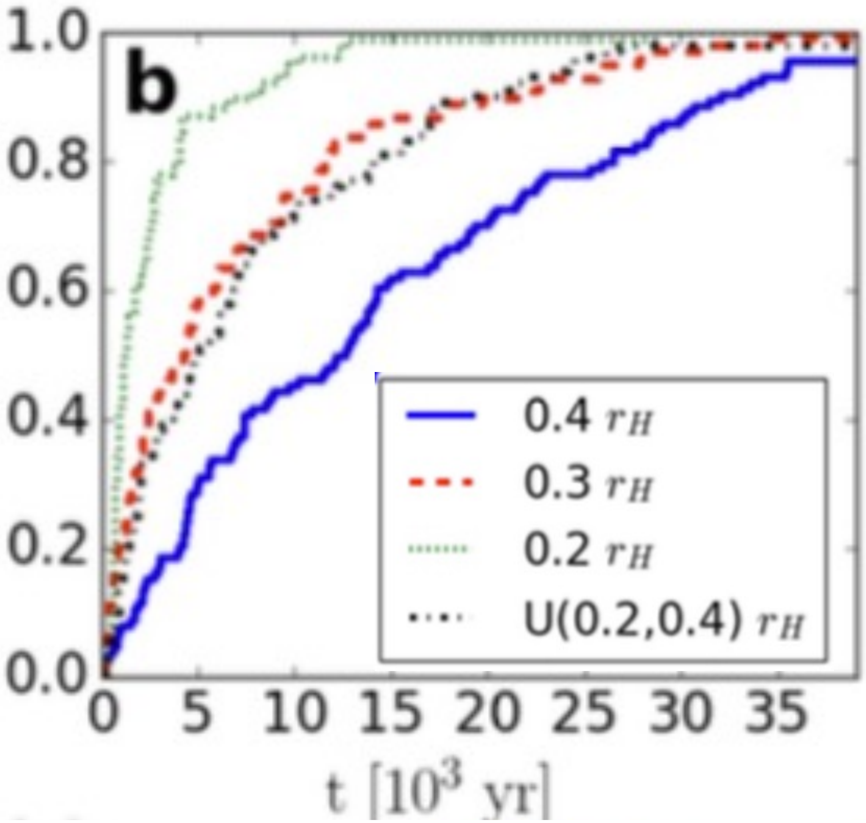

Time to contact

Too short to allow for alignment

Grishin et al. (2020)

Alignment of the Spin Vectors

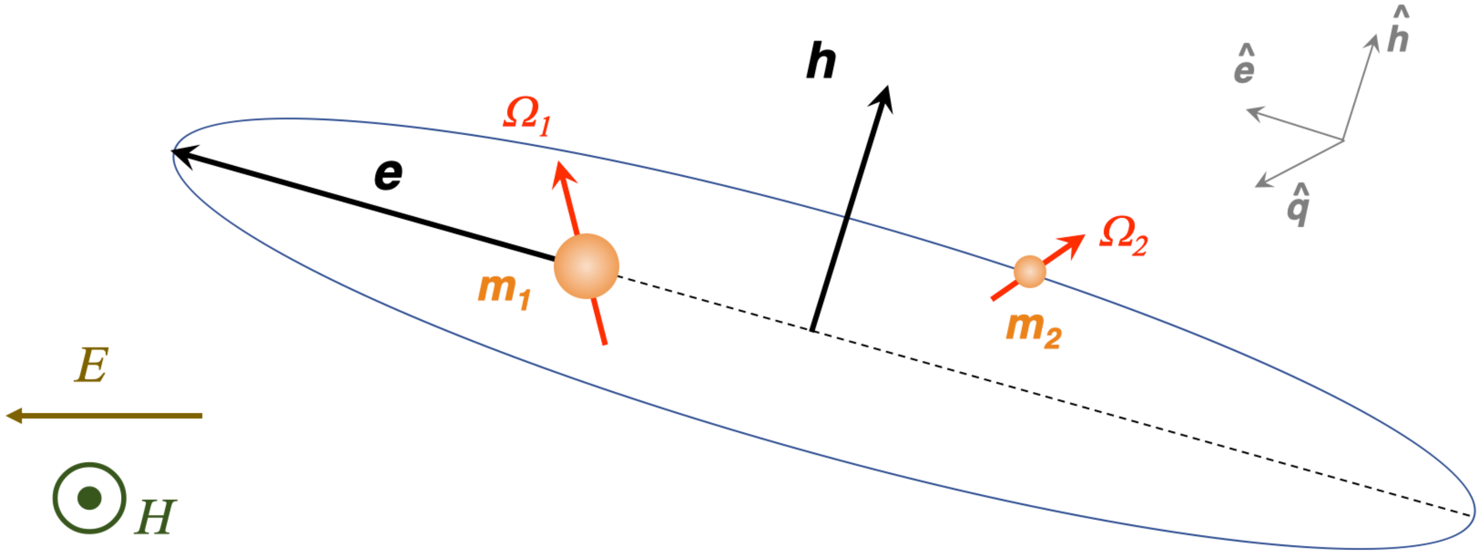

Mainly driven by J_2 (permanent quadrupole)

Timescale proportional to a^4 *(4th power of semimajor axis)*

5 Gyr for $a/R \sim 100$

0.5 Myr for $a/R \sim 10$

Lyra et al 2021

- Solved the hierarchical 3-body problem with gas drag
- Implemented the solution into a Kozai plus tidal friction code
- Contact via Kozai cycles in the Kuiper belt, orbits become grazing
- Window of contact increased by J_2 and drag
- 10% of KBCC binaries should be contact binaries
- Velocities at contact should be about 3-4 m/s

...1 January 2019.

The two bodies slowly spiral closer until they touch, forming the bi-lobed object we see today.

Lyra et al 2021

The density dichotomy of Kuiper Belt objects

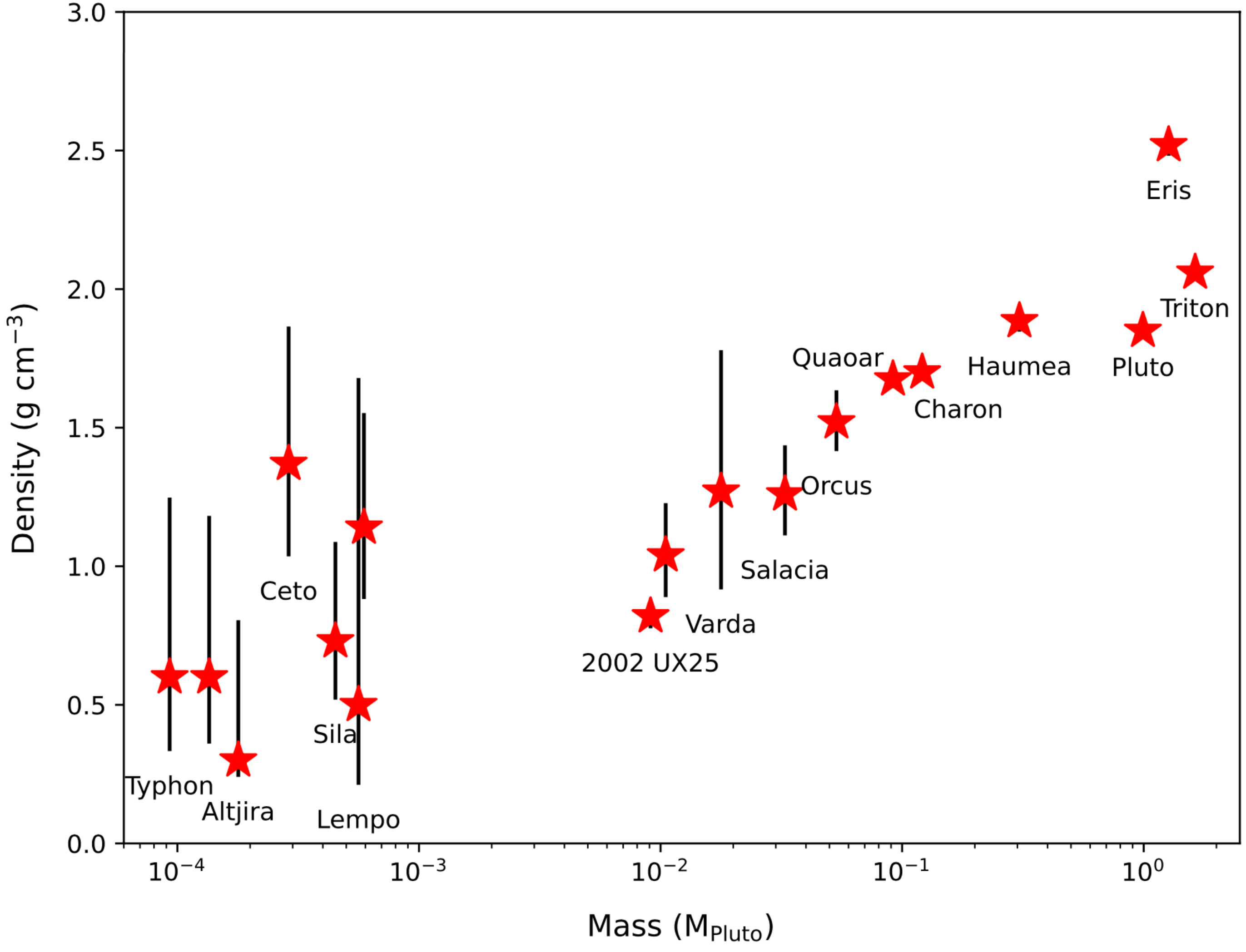

Canas+Lyra et al. 2024

Possible Solution?

- Assumptions
  - Constant composition at birth and growth
  - Porosity removal by gravitational compaction

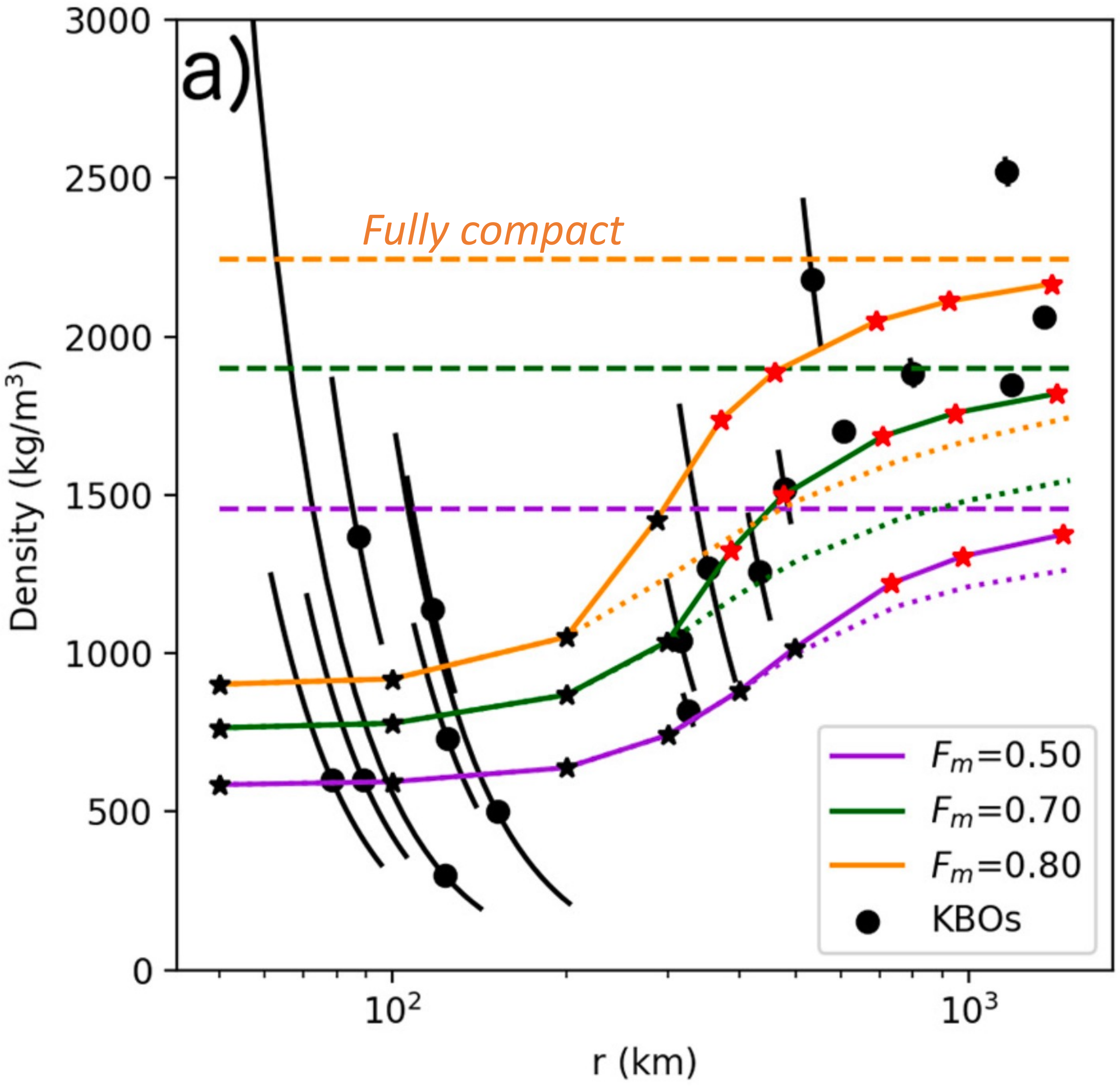

- Problems
  - Low-mass objects need to be unreasonably porous
  - Timing! ^{26}Al would melt if formed within 4 Myr

Bierson & Nimmo 2019

Abandoning Constant Composition

Heating and UV irradiation remove ice on Myr timescales

- Small grains lofted in the atmosphere lose ice
- Big grains are shielded and remain icy.

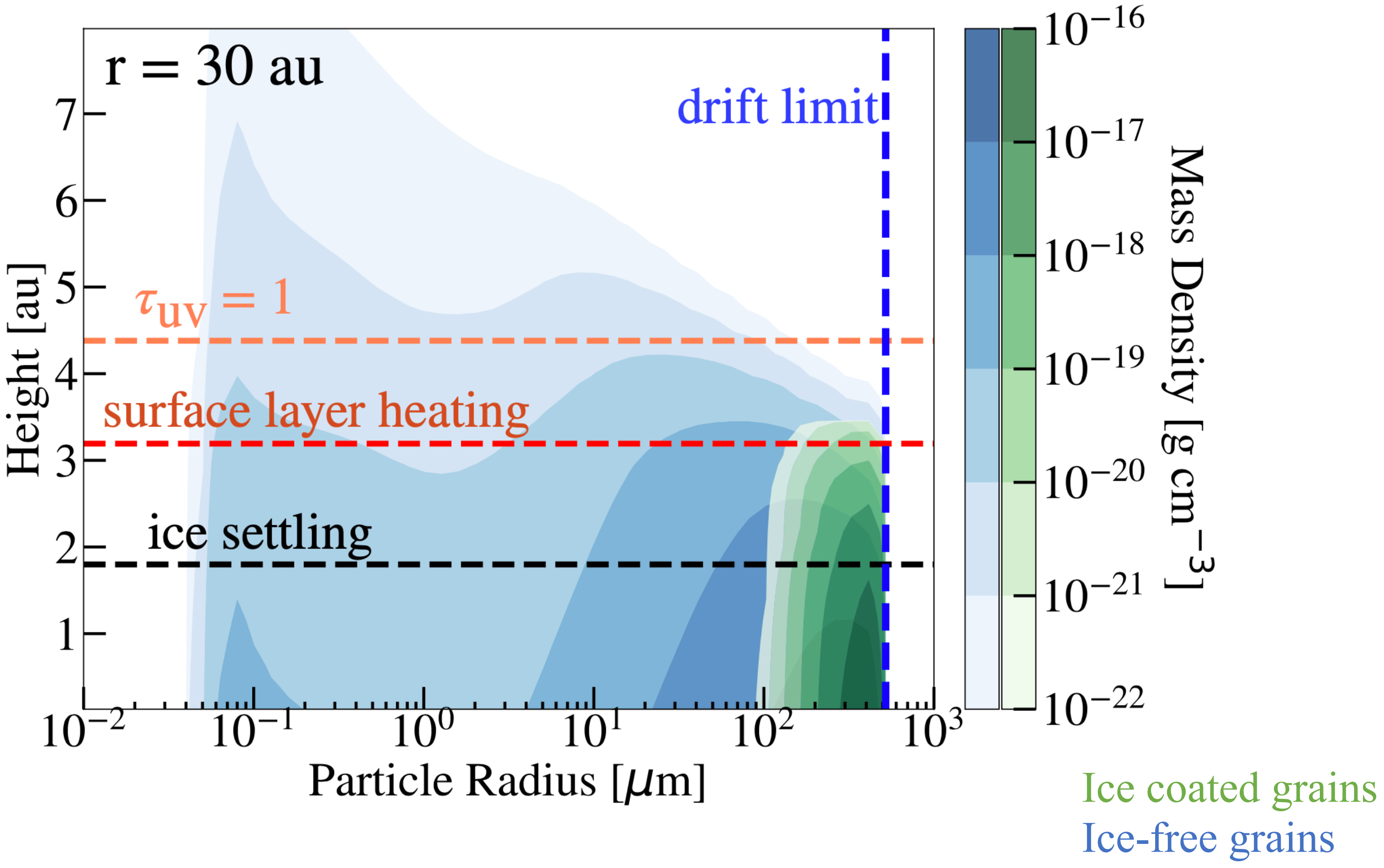

Powell et al. 2022

Split into icy and silicate pebbles

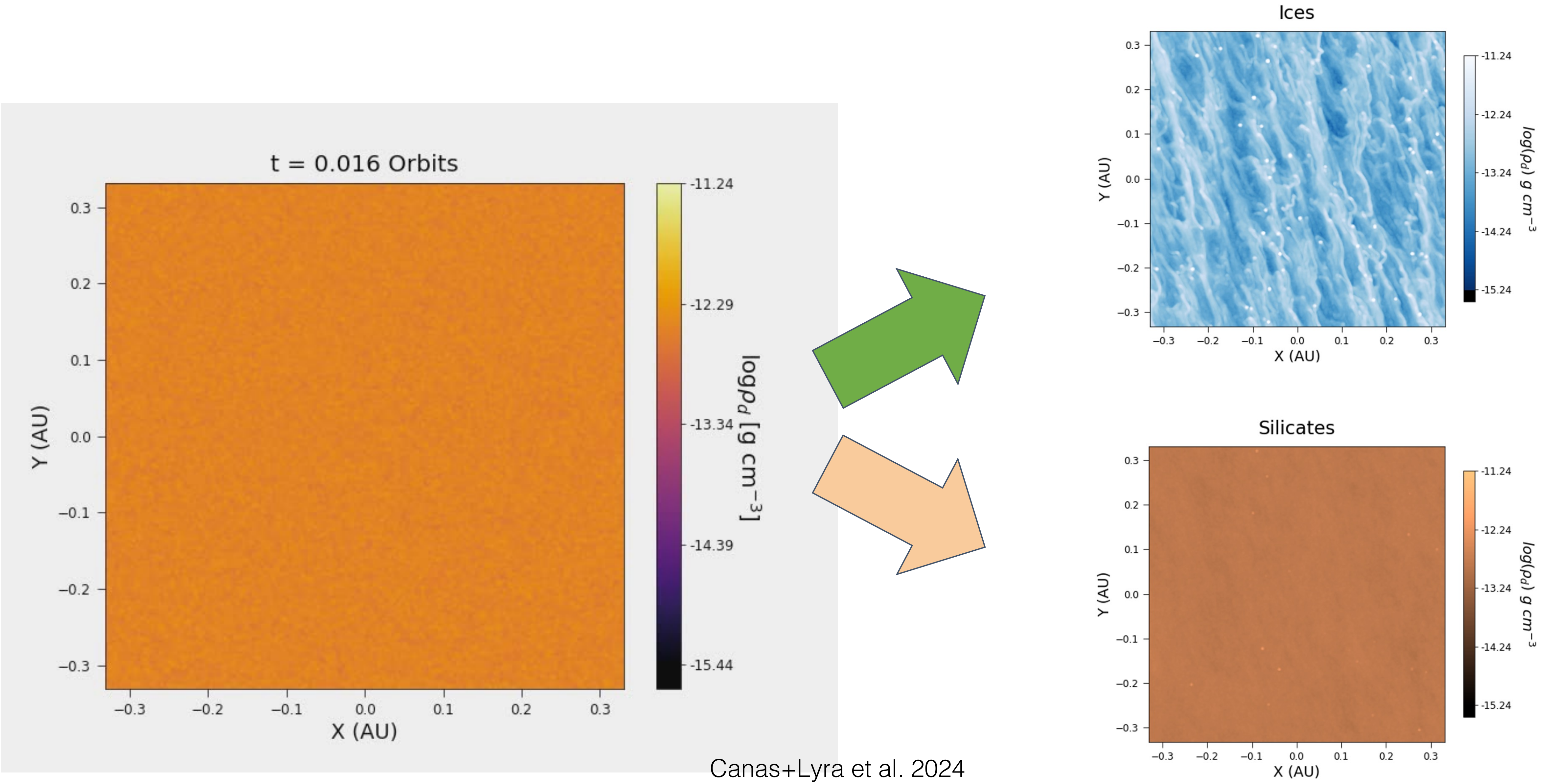

Canas+Lyra et al. 2024

The first planetesimals are icy

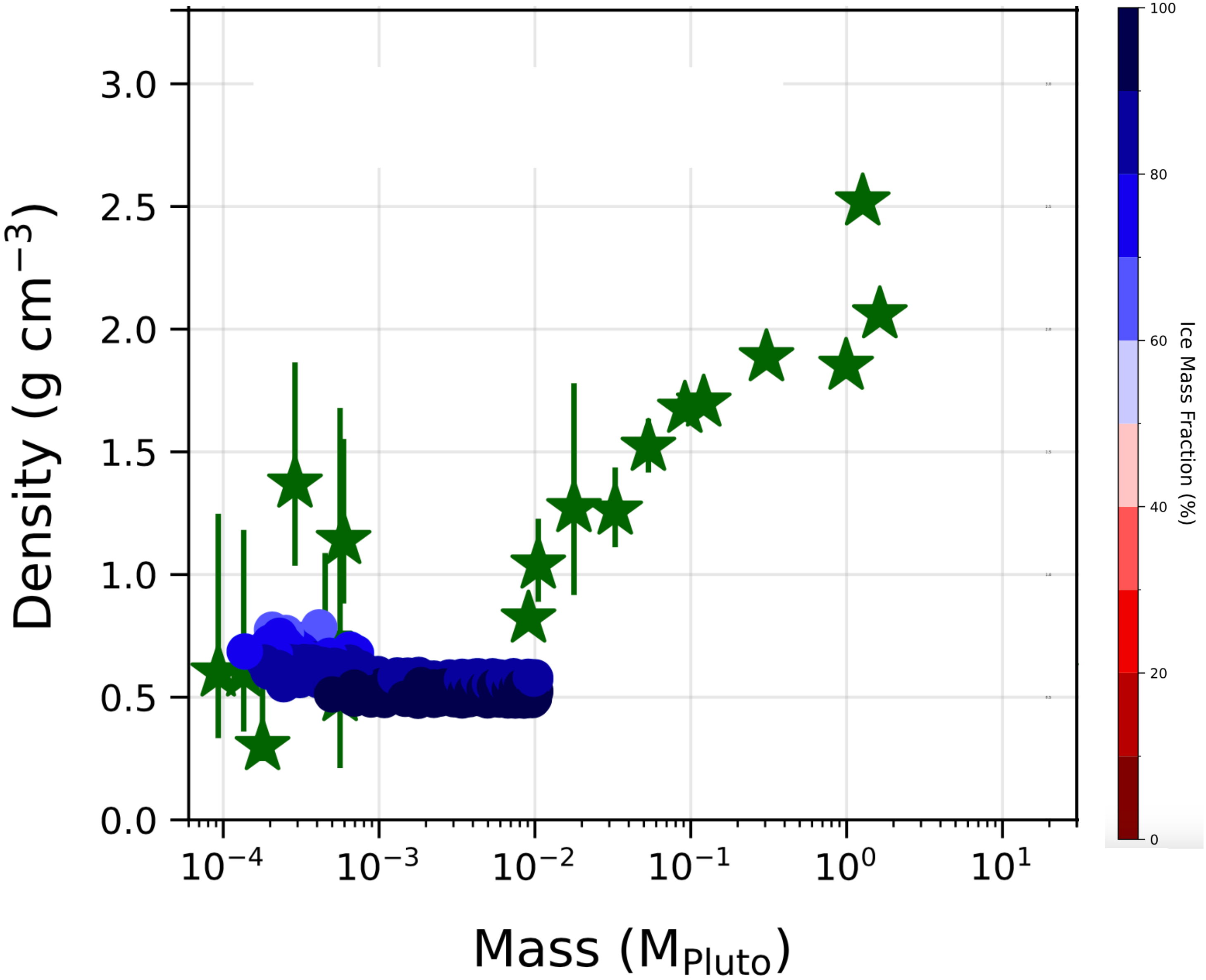

Canas+Lyra et al. 2024

Pebble Accretion

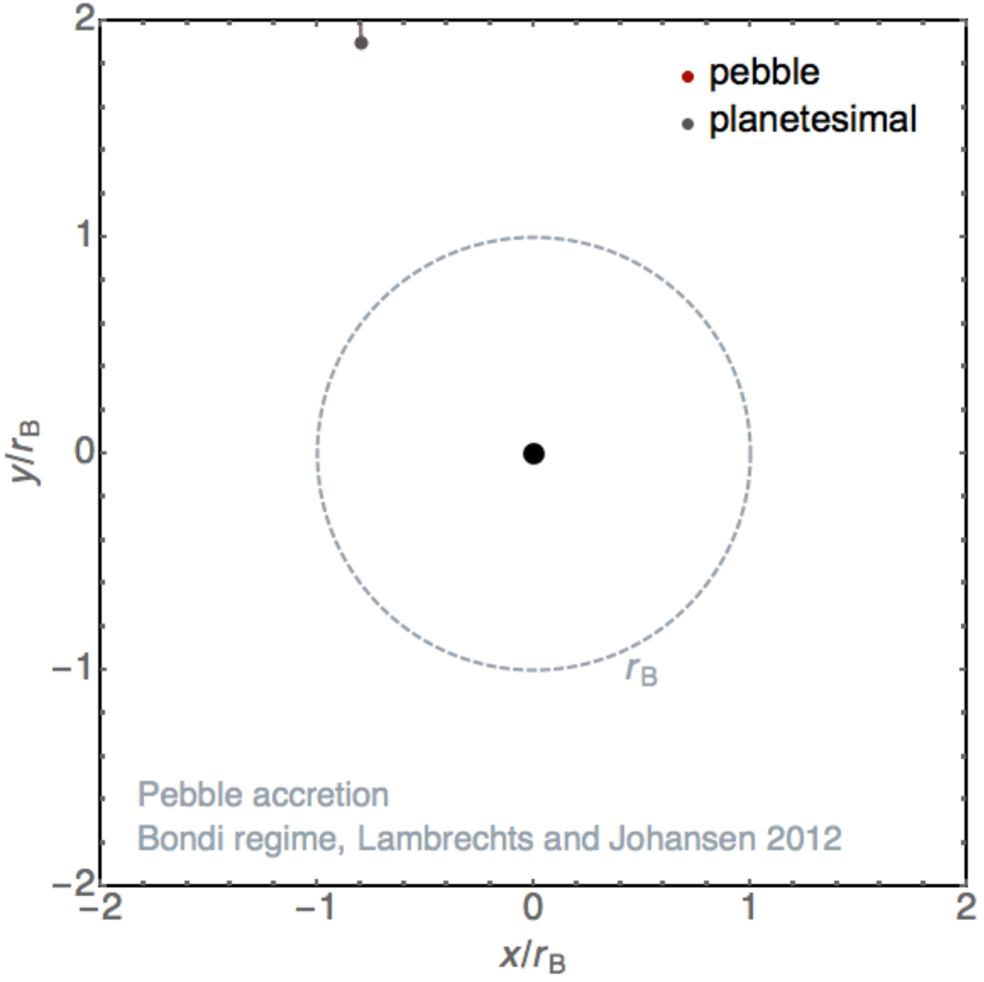

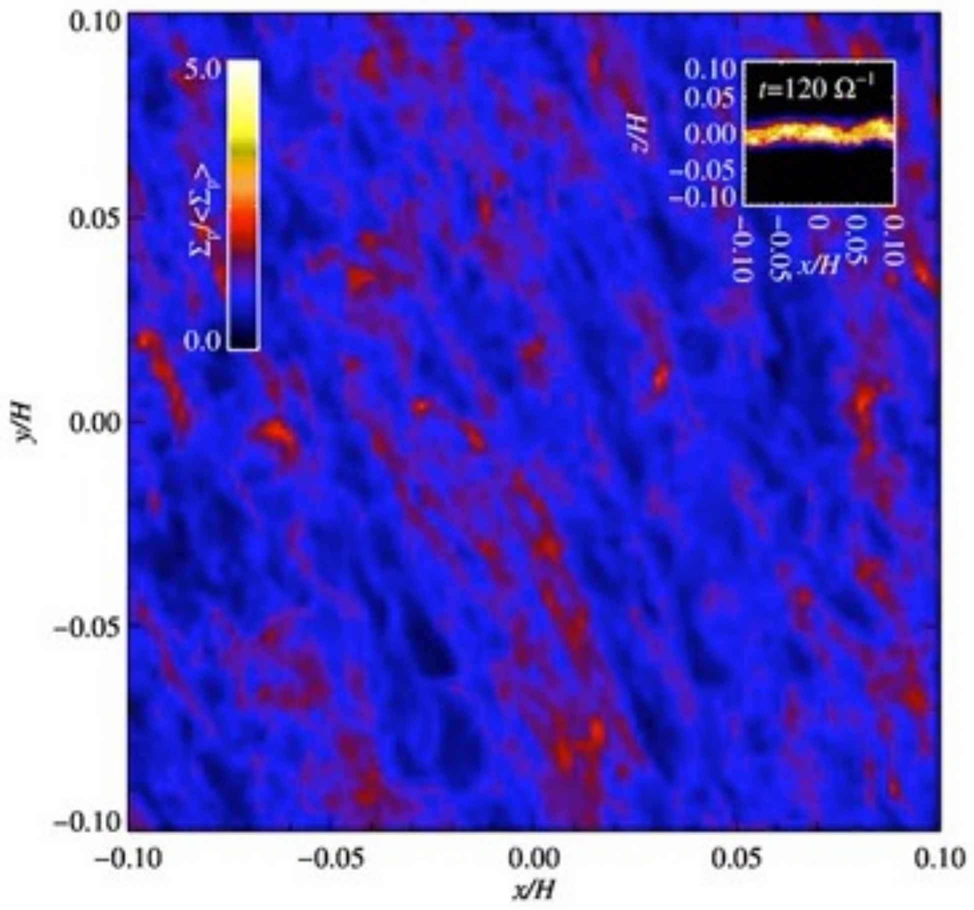

Lyra+ ‘08, ’09, ’23, Ormel & Klahr ‘10, Lambrechts & Johansen ’12
See Johansen & Lambrechts ‘17 for a review

Pebble Accretion: Geometric, Bondi, and Hill regime

$$\xi \equiv \left(\frac{R_{acc}}{2H_d}\right)^2 \qquad \dot{M}_{3D} = \lim_{\xi\to 0} \dot{M} = \pi R_{acc}^2 \rho_{d0} \delta v, \qquad \dot{M}_{2D} = \lim_{\xi\to\infty} \dot{M} = 2R_{acc} \Sigma_d \delta v,$$

Bondi accretion - Bound against thermal (dynamic) kinetic energy
Hill accretion - Bound against stellar tide

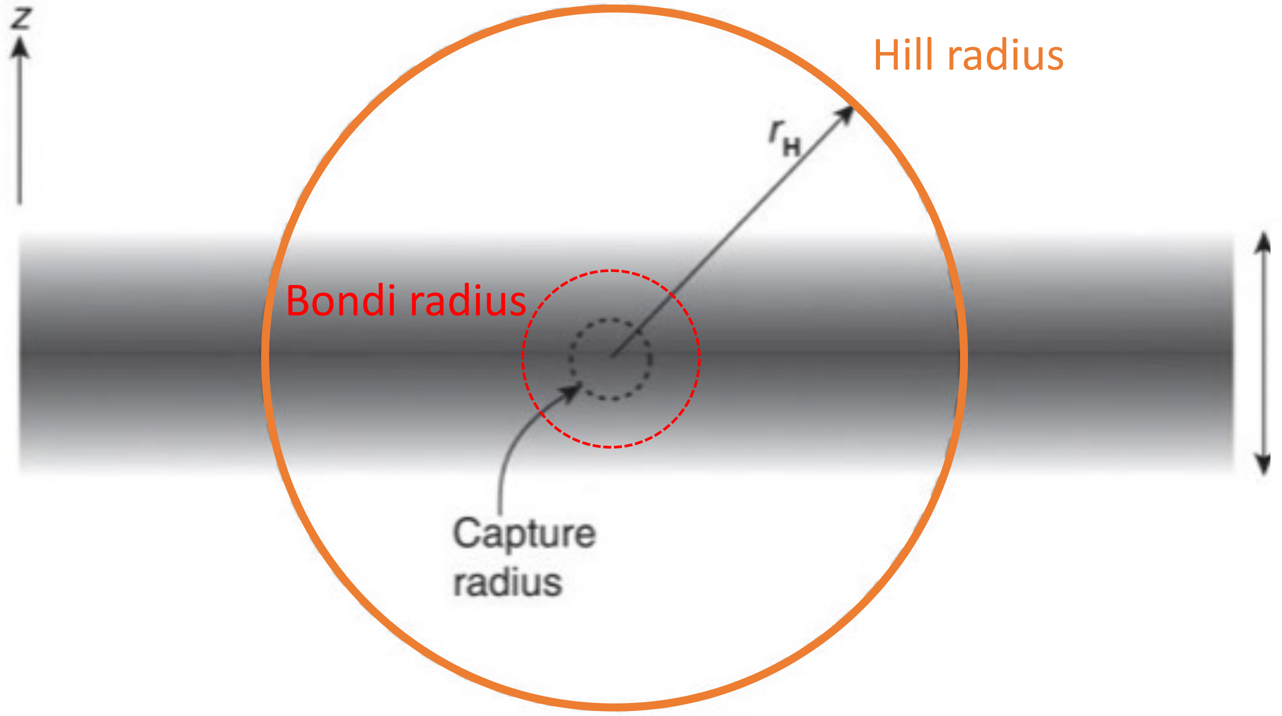

Mass Accretion rates

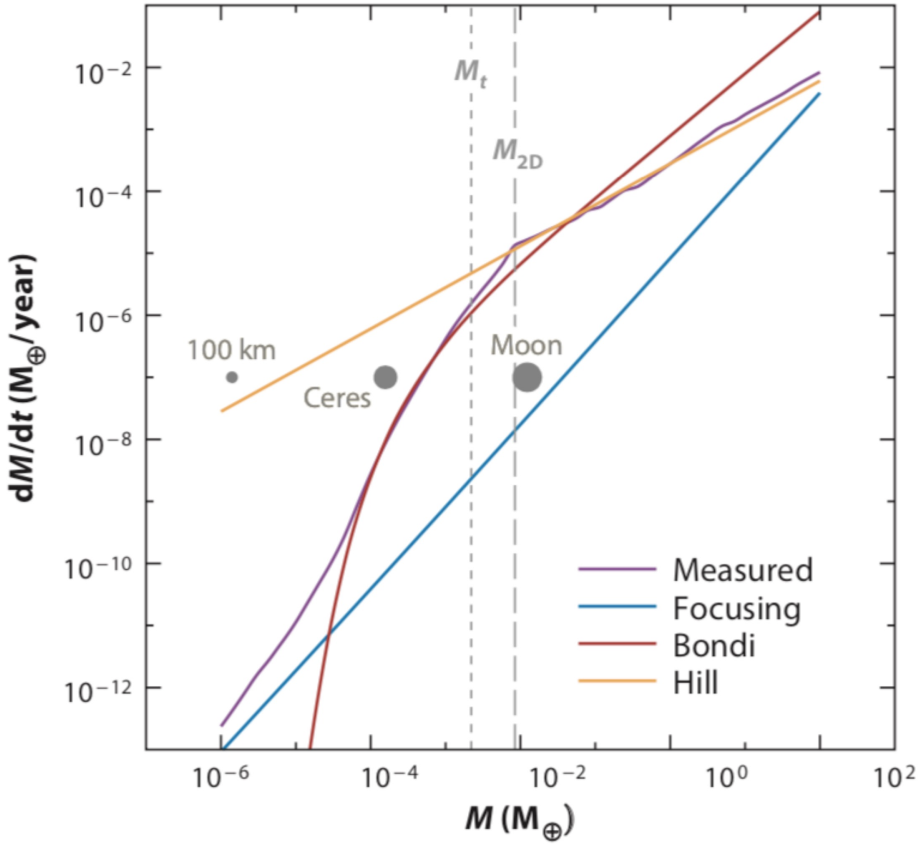

Johansen & Lambrechts '17

Integrate pebble accretion

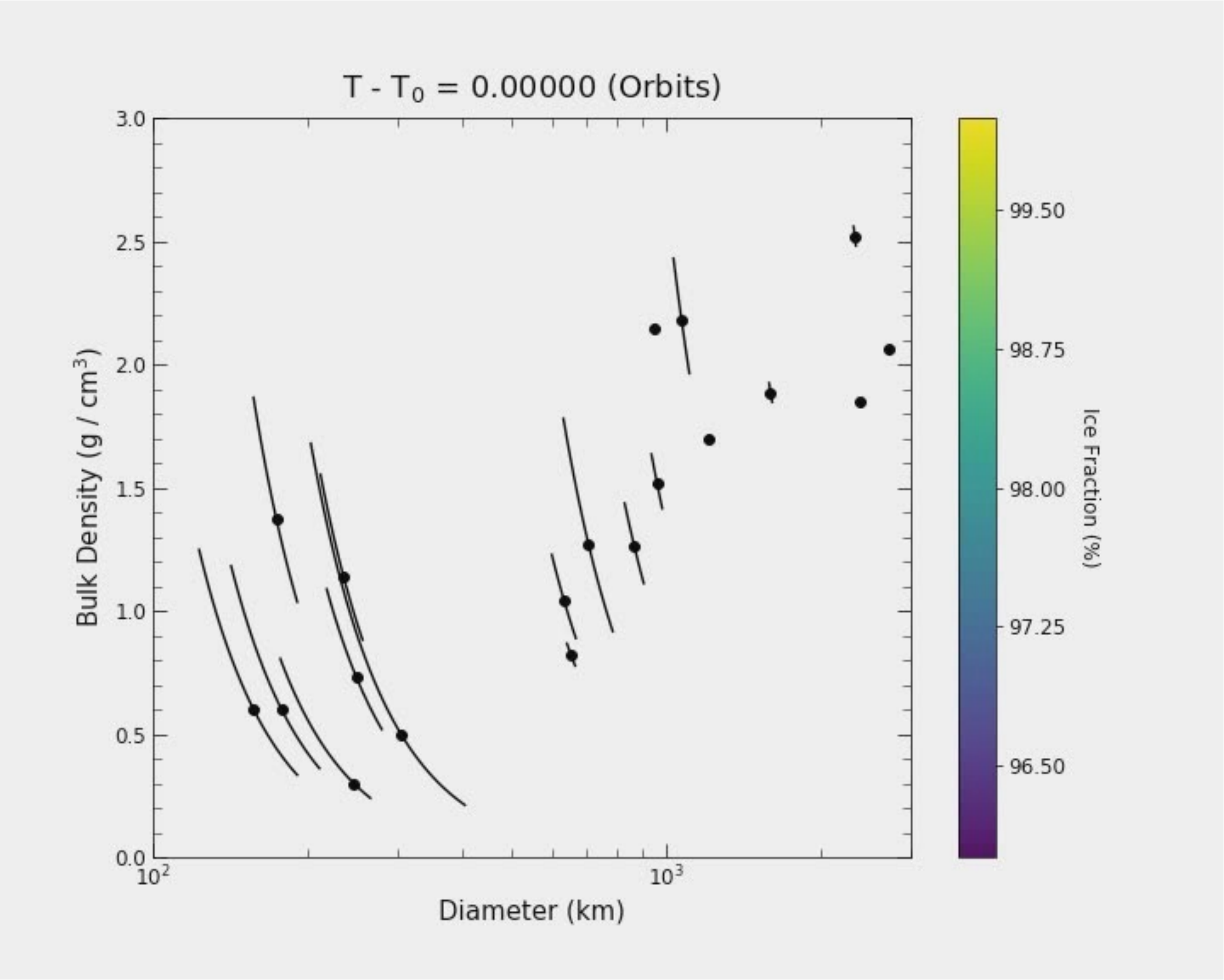

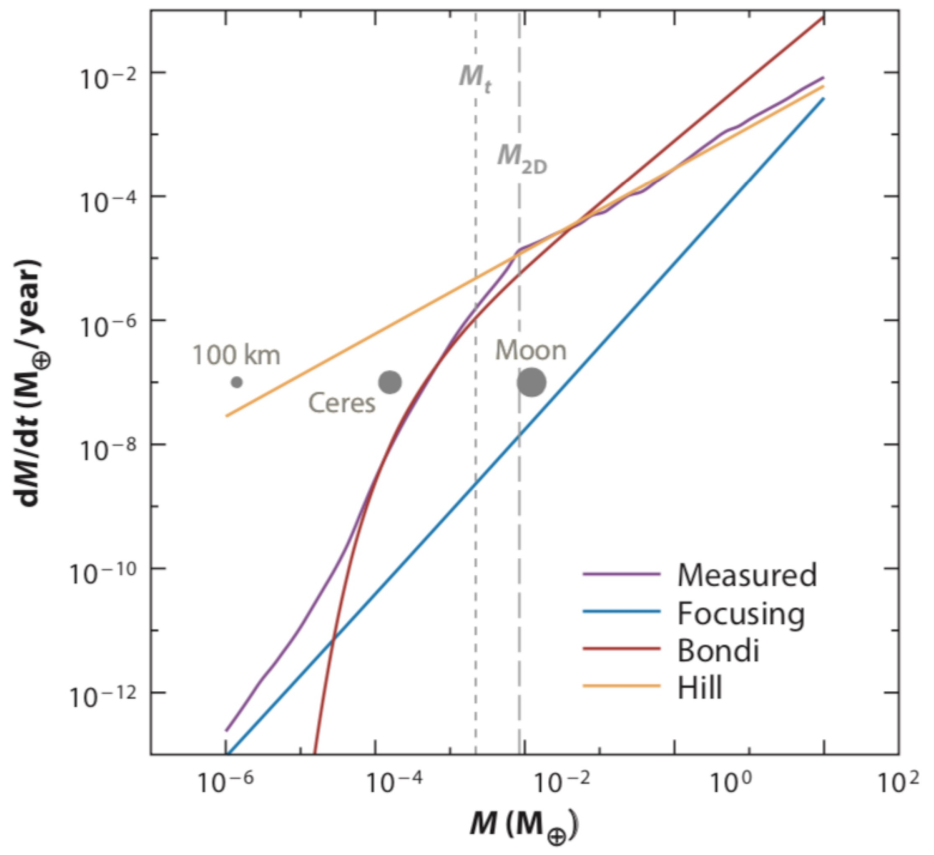

Pebble Accretion: Pebbles of different size accrete differently

Bondi Regime

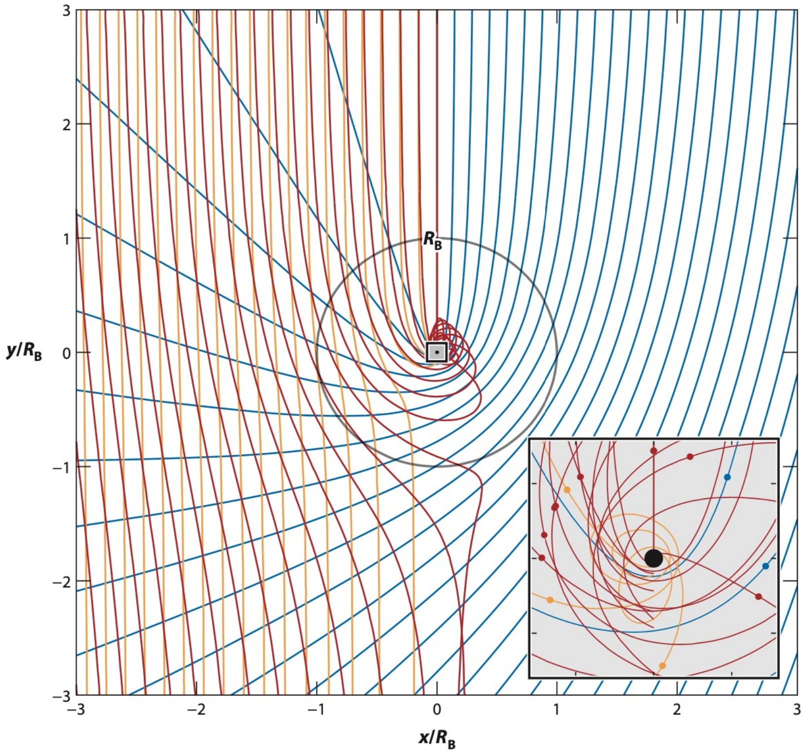

Best accreted
Drag time = Bondi Time

Hill Regime

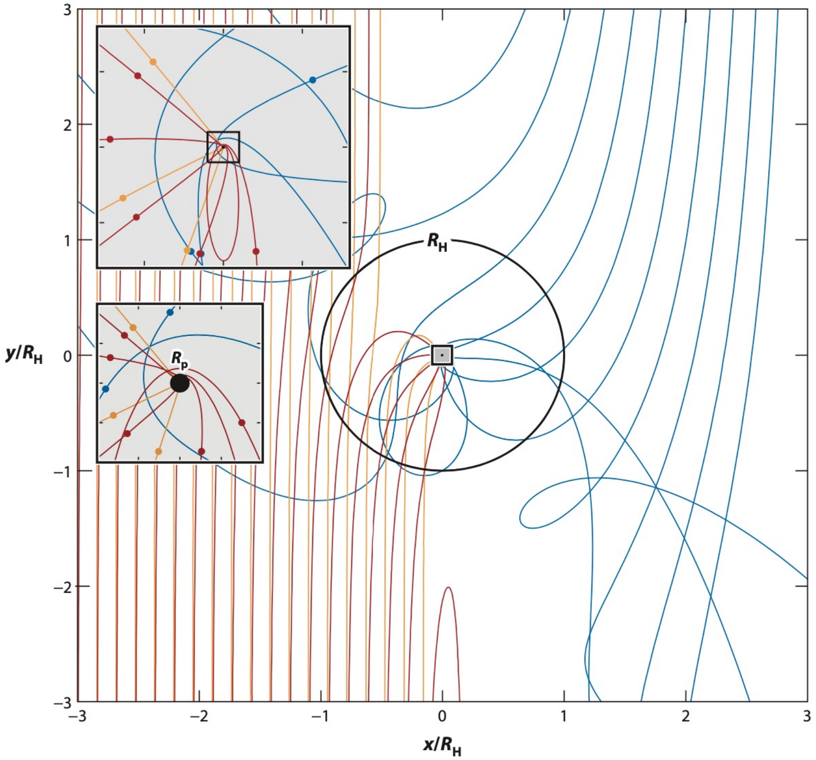

Best accreted
Drag time ~ Orbital Time

Accretion Rates

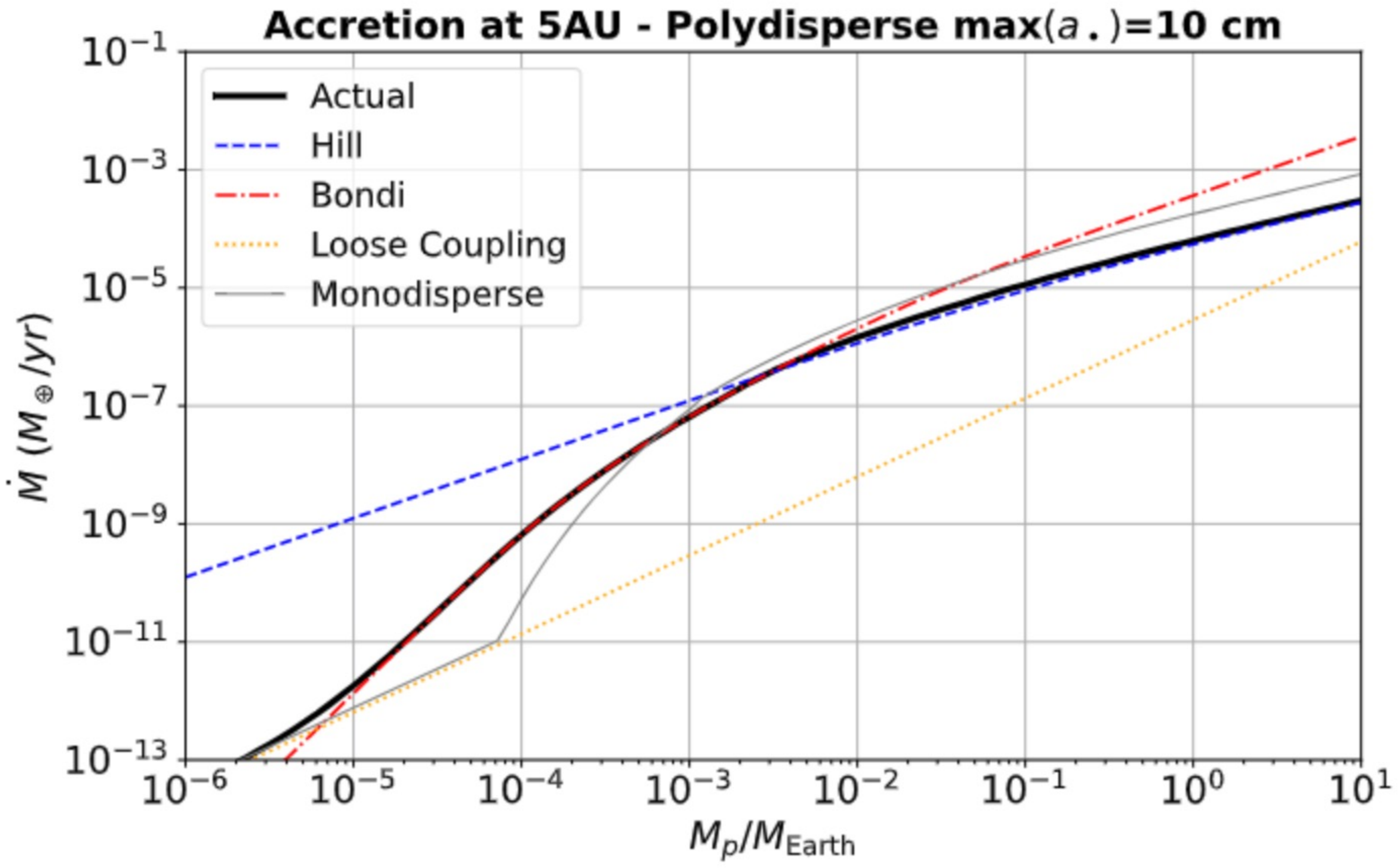

Lyra et al. 2023

Analytical theory of polydisperse (multi-species) pebble accretion

$$\xi \equiv \left(\frac{R_{\rm acc}}{2H_d}\right)^2$$

Monodisperse (single species)

$$\dot{M}_{\rm 3D} = \lim_{\xi \to 0} \dot{M} = \pi R_{\rm acc}^2 \rho_{d0} \delta v,$$

$$\dot{M}_{\rm 2D} = \lim_{\xi \to \infty} \dot{M} = 2 R_{\rm acc} \Sigma_d \delta v,$$

Lambrechts & Johansen (2012)

Polydisperse (multiple species)

$$\dot{M}_{\rm 2D,Hill} = \frac{6(1-p)}{14-5q-3k}\left(\frac{\rm St_{max}}{0.1}\right)^{2/3} \Omega R_H^2 Z \Sigma_g.$$

$$\dot{M}_{\rm 3D,Bondi} \approx C_1 \frac{\gamma_l\left(\frac{b_1+1}{s}, j_1 a_{\rm max}^s\right)}{s j_1^{(b_1+1)/s}} + C_2 \frac{\gamma_l\left(\frac{b_2+1}{s}, j_2 a_{\rm max}^s\right)}{s j_2^{(b_2+1)/s}} + C_3 \frac{\gamma_l\left(\frac{b_3+1}{s}, j_3 a_{\rm max}^s\right)}{s j_3^{(b_3+1)/s}} + C_4 \frac{\gamma_l\left(\frac{b_4+1}{s}, j_4 a_{\rm max}^s\right)}{s j_4^{(b_4+1)/s}},$$

Lyra et al. (2023)

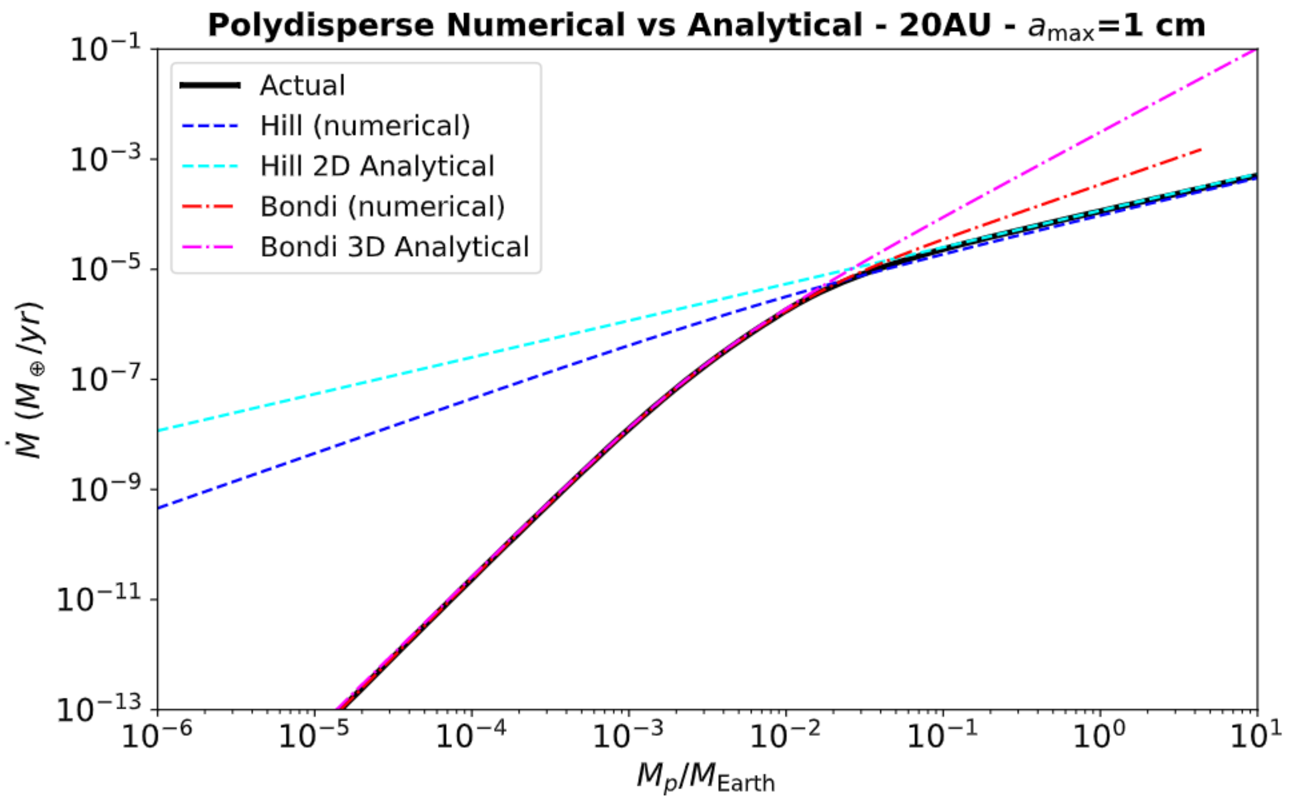

Lyra et al. 2023

Growing Pluto by silicate pebble accretion

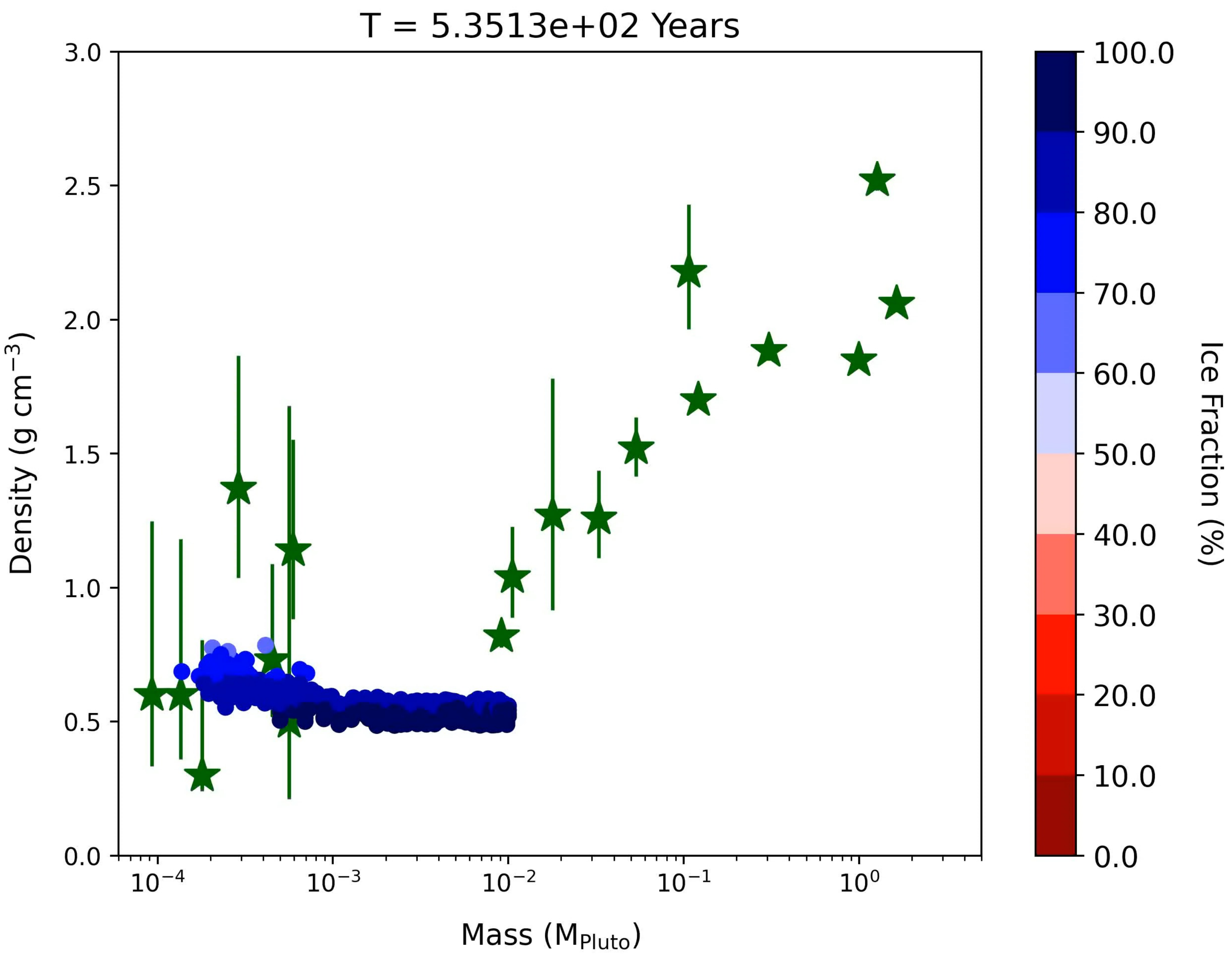

Canas+Lyra et al. 2024

Pebble Density

Ice Fraction

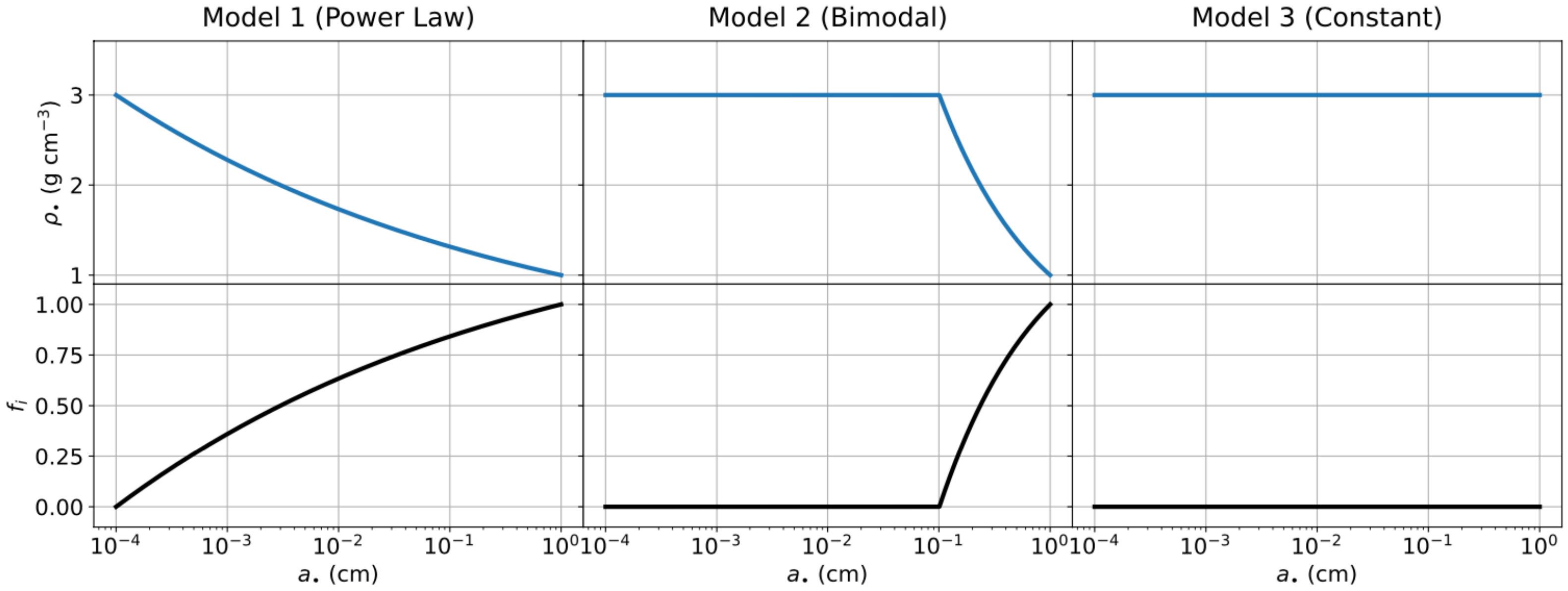

Mass Accretion rate

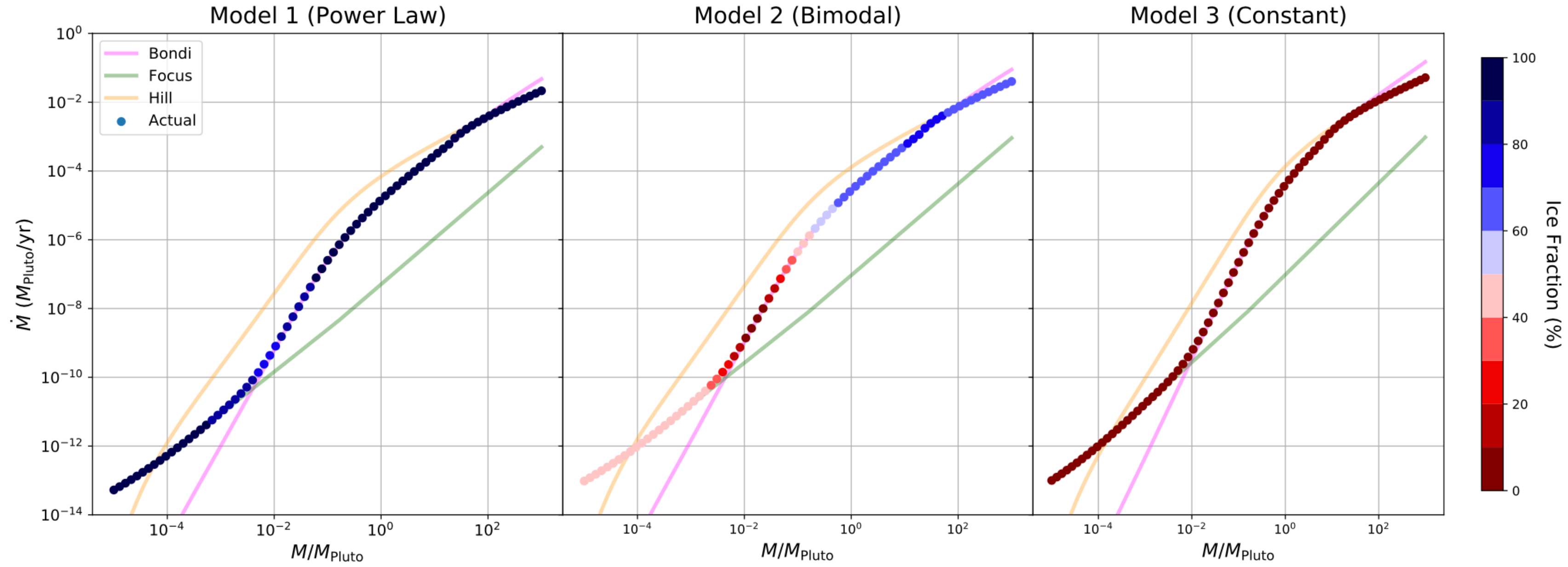

Canas+Lyra et al. 2024

Growing Pluto by silicate pebble accretion

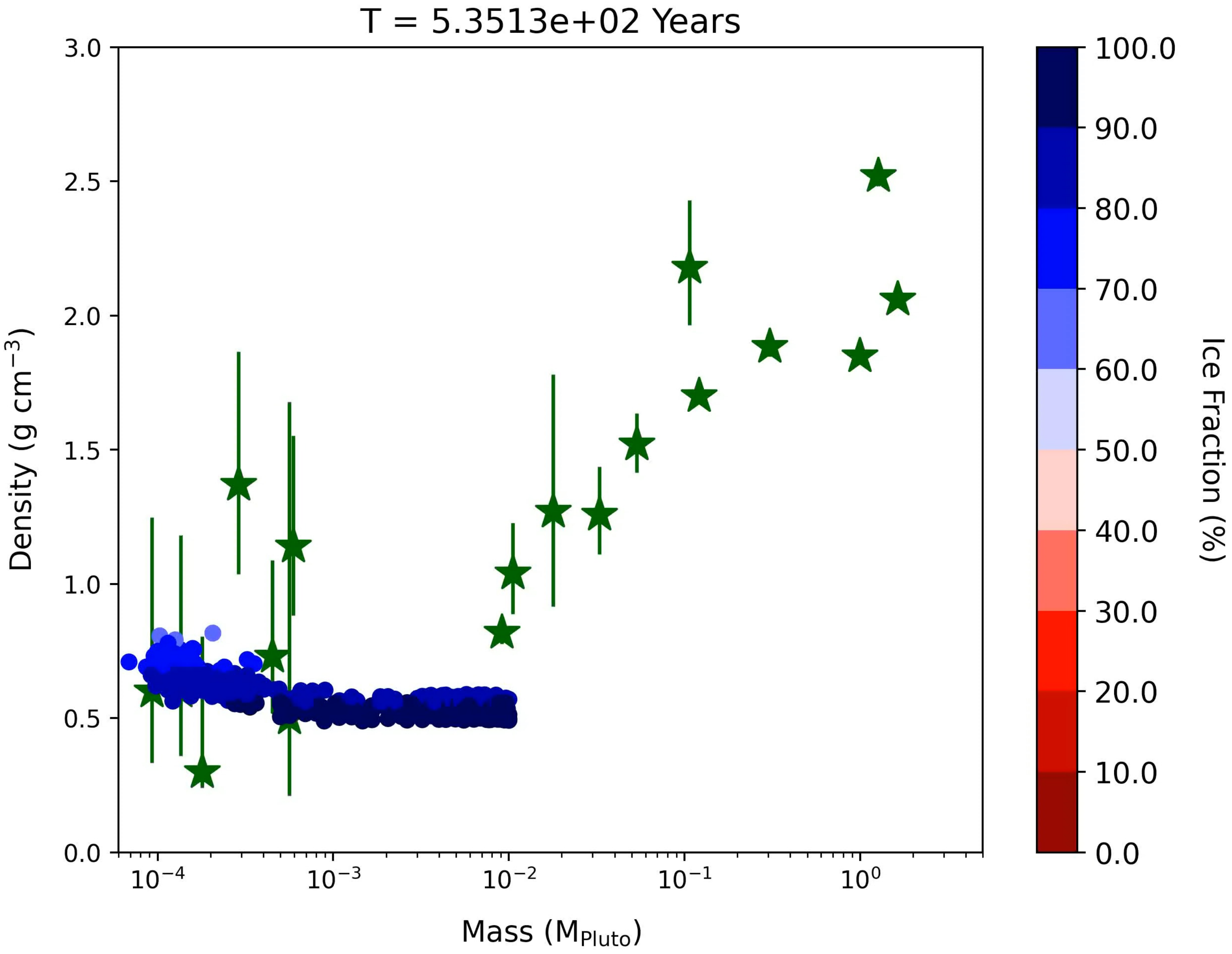

Canas+Lyra et al. 2024

Resulting Densities vs Mass relations

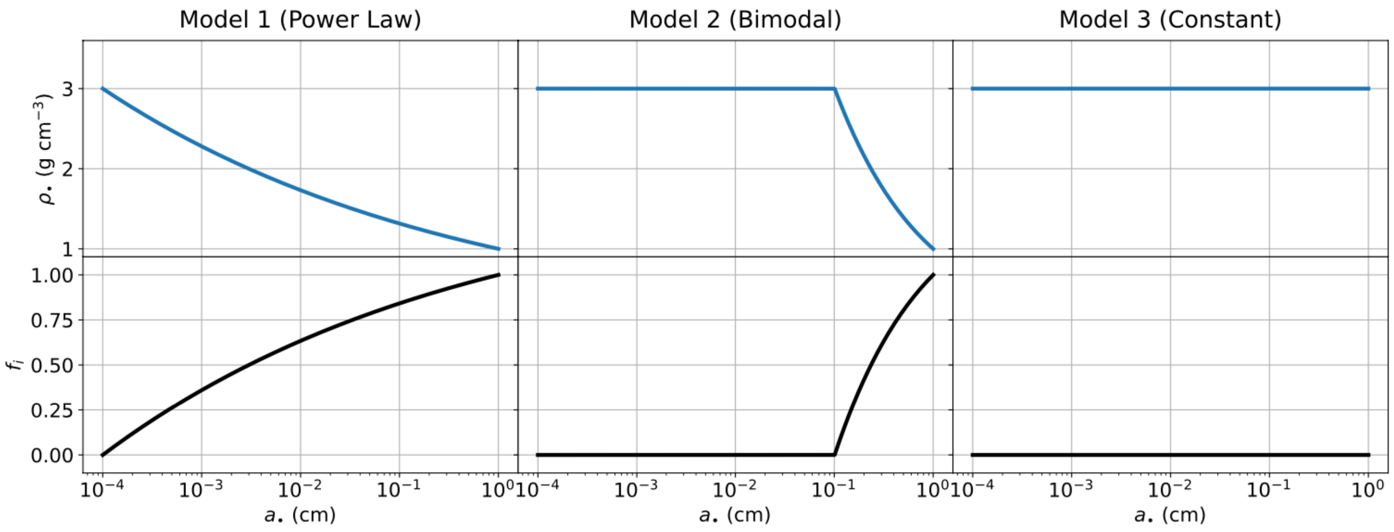

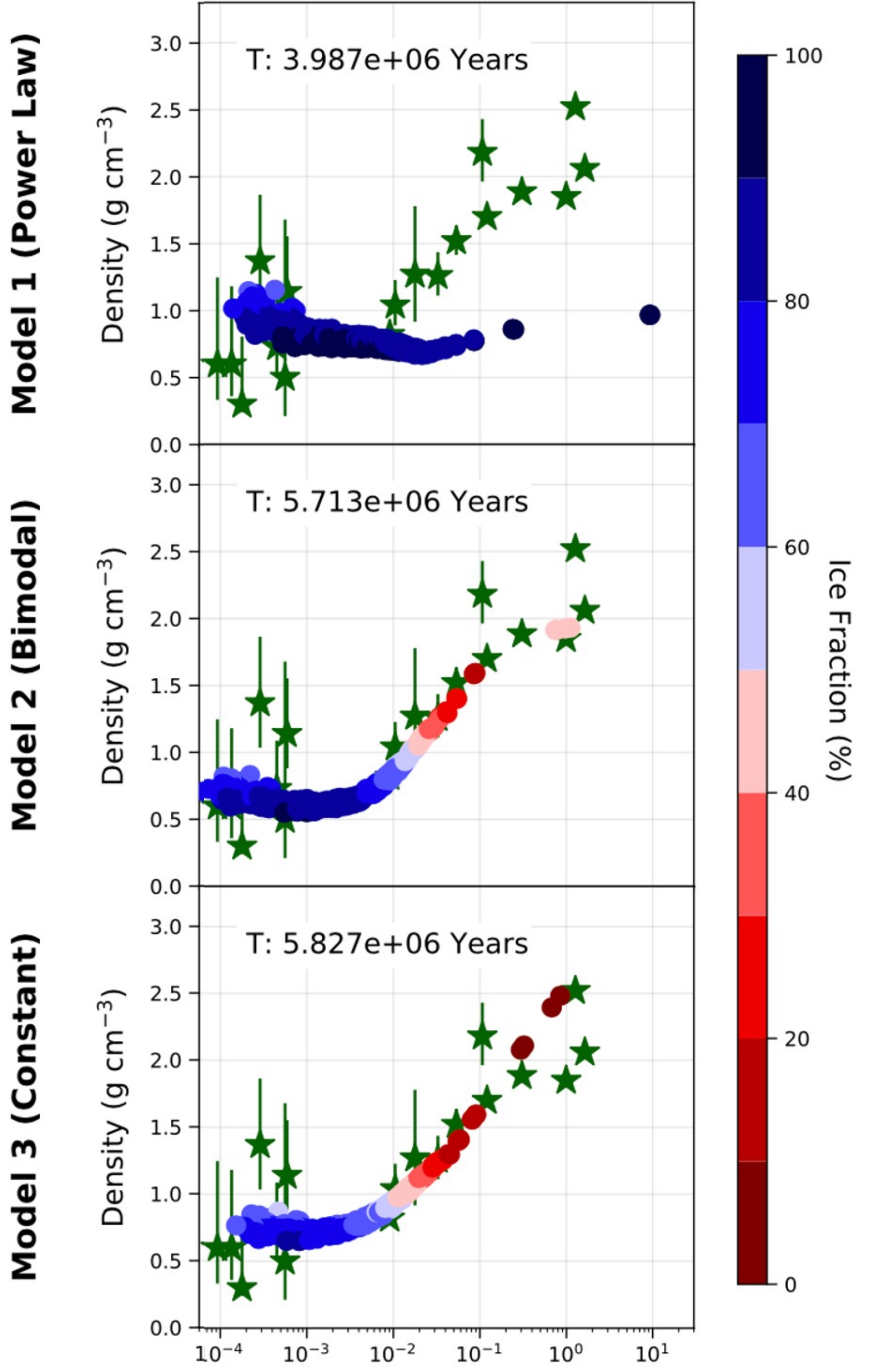

- Polydisperse Bondi accretion 1-2 orders of magnitude more efficient than monodisperse
    - Best accreted pebbles are those of drag time ~ Bondi time, not the largest ones
    - The largest ones dominate the mass budget, but accrete poorly
- Onset of Bondi accretion 1-2 orders of magnitude lower in mass compared to monodisperse
    - Reaches 100-350km objects within Myr timescales
    - Bondi accretion possible on top of Streaming Instability planetary embryos within disk lifetime
- Analytical solution to
    - Polydisperse 2D Hill and 3D Bondi

Problem: wrong number density

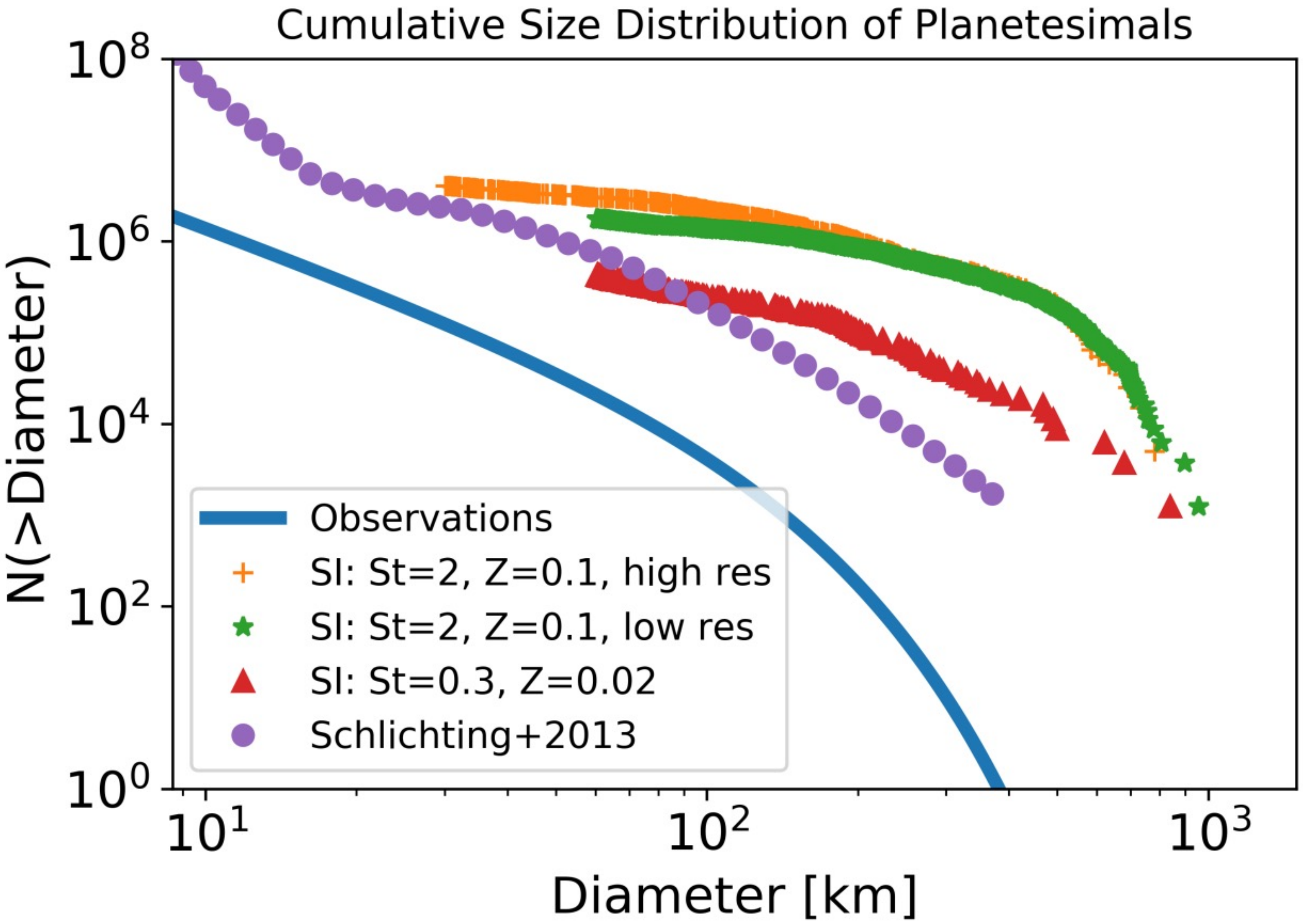

Simon et al. 2023

Conclusions

- Streaming Instability fits
  - slope of asteroid belt distribution,
  - prograde-retrograde distribution of Kuiper belt objects
  - Low density of small classical Kuiper belt objects

- Pebble accretion is a very efficient planetary growth mechanism
  - Polydisperse Bondi accretion 1-2 orders of magnitude more efficient than monodisperse
  - Silicate pebble accretion explains densities of high-mass Kuiper belt objects